ated effects rather than the presence of HBx, parental Chang liver cells were included. As in HBx-nonexpressing p34X cells, phosphorylated PTTG1 in Chang liver cells were only detected after proteasome plus PP2A inhibition independently of Dox treatment (Supporting Fig. 4A).

Additionally, we compared PTTG1 distribution between HBx-expressing versus HBx-nonexpressing cells after OA treatment by immunofluorescence experiments. Of note, not all p34X cells expressed HBx in response to Dox treatment. In the absence of OA, PTTG1 was diffusely localized in both the nucleus and cytoplasm of HBx-positive and -negative p34X cells (Fig. 5B, top). As mentioned, OA treatment reduced PTTG1 levels (Fig. 5B, bottom). However, we observed a PTTG1 accumulation in HBx-positive cells that colocalized with the viral protein. To quantify the effect of HBx on PTTG1 accumulation after OA treatment, Chang liver cells were transfected with the bicistronic plasmids pCMS-EGFP-HBx (HBx-expressing vector; CMS-X) or pCMS-EGFP (control vector; CMS-O) and processed for immunofluorescence after PP2A inhibition. As shown in Fig. 5C, there was a marked increase of PTTG1-positive cells when transfected with HBx-expressing vector compared with control vector.

It has been shown that HBx is an inhibitor of both proteasome complex[26] and ubiquitin ligases.[6] Therefore, HBx could promote PTTG1 accumulation through proteasome and/or ubiquitin ligase inhibition. Because ubiquitination targets proteins to proteasomal degradation, we analyzed the ubiquitination of PTTG1 in the presence of HBx. For this purpose, unstimulated or Dox-treated p34X cells were incubated with the proteasome inhibitor MG132 and used for immunoprecipitacion using an anti-PTTG1 Ab. Membranes were blotted with anti-ubiquitin monoclonal Ab to detect ubiquitinated forms of PTTG1. As expected, MG132-mediated proteasome inhibition promoted the accumulation of polyubiquinated PTTG1 forms in cells that did not express HBx (Fig. 5D, lane 7 versus lane 5). In contrast, incubation of HBx-expressing cells with MG132 did not significantly increase the levels of ubiquitinated forms of PTTG1 (Fig. 5D, lane 8 versus lane 6). Similar results were obtained in Hela cells cotransfected with expression vectors coding for HA-tagged ubiquitin (HA-ubiquitin), PTTG1 (pcDNA-PTTG1), and either an HBx-coding vector (pSVX) or the control plasmid (pSVHygro) (Supporting Fig. 4B). The tight junction–associated protein occludin is ubiquitinated, and its degradation is sensitive to proteasome inhibition.[27] To analyze whether HBx affected general ubiquitination events, we determined the influence of HBx on occludin ubiquitination. As shown in Fig. 5E, the accumulation of polyubiquitinated occludin was not affected by HBx expression. Together, these results strongly suggested that HBx specifically reduced PTTG1 ubiquitination.

HBx Disrupts the Interaction Between PTTG1 and the SCF Protein Complex. It has been reported that phosphorylated forms of PTTG1 are degraded by the proteasome after ubiquitination by SCF ubiquitin ligase complex.[28] In agreement with our previous results using other cell lines,[11] coimmunoprecipitation assays using lysates of unstimulated p34X cells treated with OA plus MG132 revealed that the SCF core component Cul1 coimmunoprecipitated with PTTG1 (Fig. 6A, top, lane 4). Interestingly, treatment of p34X cells with Dox to induce HBx expression partially disrupted the interaction between PTTG1 and Cul1 (Fig. 6A, lane 5 versus lane 4). GST-based pull-down assays revealed that the fusion protein GST-PTTG1, but not GST, interacted with endogenous Cul1 from a cellular lysate of noninduced p34X (Fig. 6B, top, lane 5). As above, this interaction was also reduced in the presence of HBx (Fig. 6B, top, lane 6 versus lane 5). These data suggested that HBx could reduce PTTG1 ubiquitination, at least partially, by interfering the interaction between PTTG1 and SCF. In addition, these results indicated that the interaction of HBx with PTTG1 and/or SCF complex might be operating in the disruption of PTTG1/SCF association. To further explore this issue, additional pull-down assays were performed. As shown in Fig. 6D, GST-HBx interacted with endogenous PTTG1 and GST-PTTG1 associated with HBx protein (Fig. 6B bottom, lane 6). Furthermore, an interaction between GST-HBx and Cul1 could also be demonstrated (Fig. 6D). The specificity of these GST-HBx interactions was confirmed by observing no interaction of HBx with occludin and other cell cycle–regulating proteins as cyclin B1 or STAG2/SA2 (Fig. 6D). The association between HBx and Cul1 was further confirmed by confocal double-label immunofluorescence in Chang liver p34X cells in which HBx significantly colocalized with Cul1 in dot-like structures (Fig. 6E).

HBx Does Not Affect PTTG1 Stabilization in Cul1 Knockdown Cells. The SCF ubiquitin ligase complex is involved in the degradation of phosphorylated forms of PTTG1.[10] To analyze the specific role of Cul1 on HBx-mediated PTTG1 accumulation, an siRNA-based knockdown approach was employed. First, we determined the levels of PTTG1 in Chang liver cells transiently transfected with control or Cul1-specific siRNAs, and then treated or not with OA and/or MG132. Western blot analysis revealed that Cul1 knockdown promoted PTTG1 accumulation in both control and OA-treated cells. Additionally, OA treatment of Cul1 knockdown

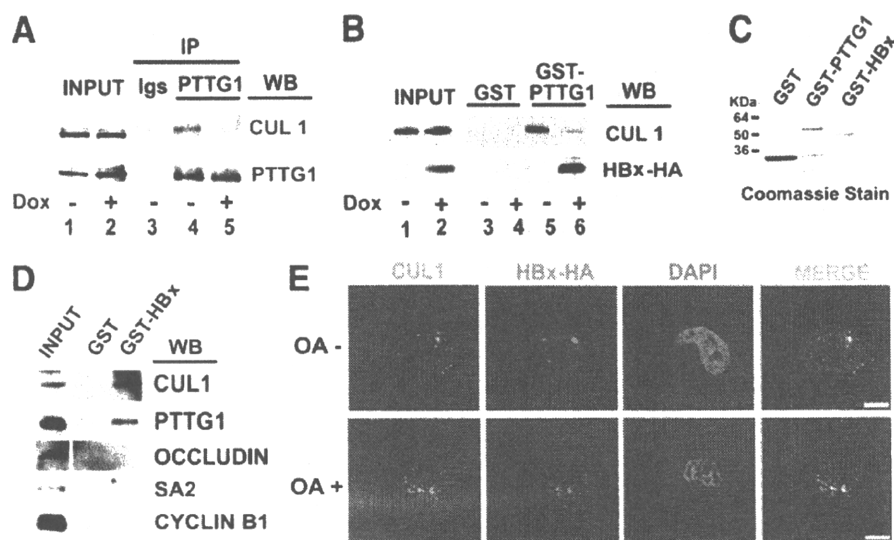

Fig. 6. HBx inhibits the interaction between PTTG1 and SCF complex. (A) Lysates from p34X cells, grown with or without Dox for 48 hours, were immunoprecipitated (IP) using anti-PTTG1 or rabbit immunoglobulin G as a control. Western blot analysis of cell lysates and immunoprecipitates was performed with anti-Cul1 (top) or anti-PTTG1 (bottom) Abs. (B) Pull-down assay with GST or GST-PTTG1 and Dox-treated (+) or untreated (−) p34X extracts. Cell lysates and bound proteins were subjected to western blotting using anti-Cul1 (top) or anti-HA (bottom) Abs. (C) Coomassie brilliant blue staining of 1/10 of the GST proteins used is shown. Molecular weight markers (kDa) are indicated on the left. (D) Pull-down assay with GST or GST-HBx and noninduced p34X cell extracts. Cell lysates and bound proteins were subjected to western blot analysis using anti-Cul1, anti-PTTG1, anti-occludin, anti-SA2, and anti-cyclin B1 Abs. (E) Confocal immunofluorescence analysis of the distribution of Cul1 (green; monoclonal Ab anti-Cul-1) and HBx (red; byotinilated Ab anti-HA epitope) in OA-treated (OA+) or untreated (OA−) p34x cells. 4',6-Diamidino-2-phenylindole staining is shown in blue. Bar = 7.5 μm. All results are representative of at least two independent experiments.

cells resulted in the formation of phosphorylated PTTG1 forms (Supporting Fig. 5). We then analyzed the effect of HBx expression on PTTG1 accumulation in Cul1-silenced cells. In both Chang liver and p34x cells, PTTG1 expression levels were increased after Cul1 silencing (Fig. 7). As above, Dox-induced HBx increased PTTG1 levels in p34X control siRNA-treated cells (Fig. 7, lane 7 versus lane 5). Interestingly, PTTG1 accumulation after Cul1 silencing was not further enhanced by HBx (Fig. 7, lane 8 versus lane 6), suggesting that the stabilization of PTTG1 by HBx was Cul1-dependent, not being likely that other ubiquitin ligase was involved. Given that HBx expression mimicked the effects of Cul-1 knockdown on PTTG1, it can be hypothesized that HBx interferes Cul1-asscociated functions. Overall, these data strongly suggest that HBx promotes the disruption of the PTTG1/SCF association and prevents its ubiquitination and subsequent degradation by the proteasome (Fig. 8).

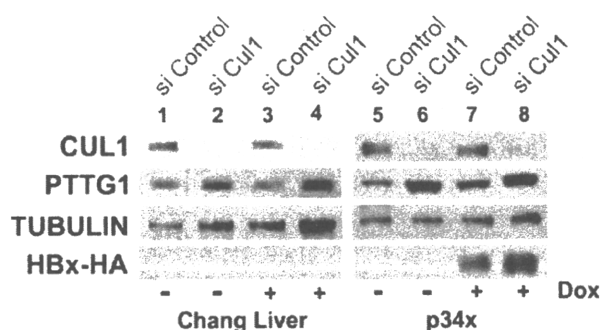

Fig. 7. HBx does not enhance PTTG1 stabilization after Cul1 knockdown. Chang liver and p34x cells were transfected with control or Cul1 siRNA and treated with Dox for 48 hours. PTTG1, Cul1, and tubulin protein levels were analyzed by means of western blotting. Results are representative of two independent experiments.

Discussion

HBV-associated carcinogenesis is a multifactorial process. Liver inflammation results in hepatocellular death and regeneration processes that lead to the accumulation of critical mutations in the host genome. In addition, the regulatory protein HBx has been involved in hepatocarcinogenesis by altering cellular processes. In the present study, we have demonstrated that PTTG1 expression levels increase in HBx-immunoreactive cells as chronic hepatitis B progresses to cirrhosis and HCC. Furthermore, PTTG1 expression increases as HBx transgenic mouse livers progress through hyperplasia to HCC. In addition, PTTG1 accumulates in human and mouse HBx-expressing cell lines and in HBV replicon-containing cells, but not in cells harboring an HBx-defective genome construct. Together, these data strongly suggest that PTTG1

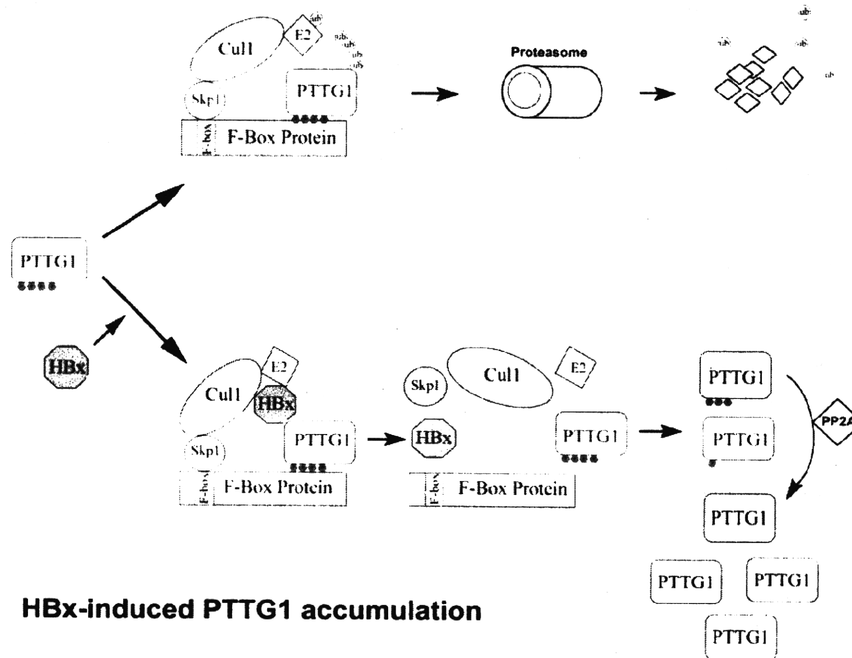

Fig. 8. Possible mechanism for HBx-mediated PTTG1 stabilization. (A) PTTG1 undergoes proteasomal degradation via ubiquitination by the SCF ubiquitin ligase complex (A. PTTG1 degradation). Cul1 interacts with PTTG1, and in the presence of HBx this interaction is disrupted. As a result, there is an impairment of PTTG1 ubiquitination that leads to an increase of its half-life (B. HBx-induced PTTG1 accumulation). The proliferative actions of PTTG1 and HBx could act synergistically in cell transformation.

accumulation is, at least partially, an HBx-mediated effect.

Several viruses, including HBV, have the ability to stimulate the cell cycle progression in order to facilitate their own replication. In doing so, viruses generally disrupt the normal cell cycle checkpoints and in turn extend proliferative signals to host cells to establish a carcinogenic environment.[29] HBx has been demonstrated to suppress serum dependence for cell cycle activation.[30] Furthermore, HBx has been shown to promote transit through G1 in G0-arrested cells and to alter G1-to-S and G2-to-M progression.[17,22] However, in Chang liver p34X cells, the cell cycle profile was unaffected after HBx induction.[24] In addition, it is known that HBx transcriptionally induces the expression of viral and cellular genes.[2] However, our data strongly suggest that HBx-promoted PTTG1 protein accumulation is not strictly dependent on cell cycle modifications or transcriptional up-regulation.

Through interactions with host factors, HBx alters different cellular processes implicated in the development of HCC. Protein degradation by the proteasome complex is a strictly regulated key event of cellular homeostasis. Oncogenic viruses alter the proteasomal activity of target cells, affecting viral entry, replication, and release and enhancing cell survival.[31] Targeting of proteins to the proteasome through interactions with ubiquitin ligases is essential for normal protein turnover. In this context, HBx is able to down-regulate both proteasome[26] and ubiquitin ligase functions.[6] Our data show that HBx induces a marked accumulation of PTTG1 protein by reducing its ubiquitination and subsequent degradation.

It has been demonstrated that the SCF ubiquitin ligase complex is involved in the degradation of phosphorylated forms of PTTG1 in nonmitotic cells. In addition, HBx affects SCF ubiquitin ligase functions through mechanisms involving protein–protein interactions.[6] Confocal microscopy analysis and biochemical data strongly suggest that HBx may interact with both the SCF component Cul1 and PTTG1. Interestingly, the association between PTTG1 and Cul1 is disrupted in the presence of HBx. However, HBx expression does not enhance PTTG1 accumulation after Cul1 silencing. Together, these data suggest that HBx may alter the formation of the SCF/PTTG1 complex, leading to an impairment of PTTG1 ubiquitination. Thus, in the presence of HBx, PTTG1 is not targeted to proteasome-mediated degradation resulting in an abnormal protein accumulation (Fig. 8). It is tempting to speculate that by affecting the normal turn-

over of PTTG1, HBx could alter some of the PTTG1-related functions and promote cellular transformation.

The SCF ubiquitin ligases are mammalian cullin RING ubiquitin ligases in which F-box proteins provide the substrate targeting specificity of the complex . Skp2 is the F-box protein that targets key regulatory proteins, such as c-myc, for degradation.[32] Interestingly, it has been shown that HBx is able to block ubiquitination of c-myc through a direct interaction with Skp2 and destabilization of the SCF/Skp2 complex. An association between HBx-mediated PTTG1 stabilization and HBx/Skp2 interaction may also exist, but this issue requires further study.

PP2A is an important serine/threonine phosphatase family involved in essential cellular processes such as cell division, gene regulation, protein synthesis, and cytoskeleton organization. PP2A enzymes typically exist as heterotrimers comprising a common catalytic subunit (PP2Ac) and different structural and regulatory subunits.[33] It has been shown that hepatotropic viruses, including hepatitis C virus and HBV, alter PP2Ac activity.[34] HBx protein is the most likely candidate responsible for HBV-mediated PP2Ac modulation.[34] Our results show that HBx promotes PTTG1 accumulation, inhibiting the degradation of phosphorylated forms of PTTG1 after chemical inhibition of PP2A. Further experiments are necessary to analyze whether HBx could affect PTTG1 expression levels by up-regulating PP2A activity.

Several lines of evidence suggest that an important transforming mechanism underlying PTTG1 overexpression is the induction of chromosomal instability.[9] Thus, it has been demonstrated that PTTG1 accumulation inhibits mitosis progression and chromosome segregation, but does not directly affect cytokinesis, resulting in aneuploidy.[35] It has been shown that HBx can transform cultured cells[21] and induce liver cancer in transgenic mice.[36] Genetic instability is frequently accompanied with the acquisition of transformation ability and malignant progression of tumors. Moreover, recent reports have shown that HBx expression induces chromosomal aberrations such as chromosome rearrangements and micronuclei formation.[37] Furthermore, HBx promotes multipolar spindle formation and chromosomal missegregation during mitosis, and increases multinucleated cells.[18] Interestingly, it has been determined that HBx binds to BubR1, a component of the mitotic checkpoint complex, and attenuates the association between BubR1 and CDC20, an activator of the anaphase-promoting complex/cyclosome, resulting in chromosomal instability.[38] Our results demonstrate that HBx induces the accumulation of PTTG1 in interphase cells. Further experiments are necessary to study the effects of HBx on PTTG1 functions during mitotic events.

In conclusion, we propose that HBx promotes alterations of PTTG1 expression levels, which may improve our understanding of the molecular mechanisms of HBV-related pathogenesis of progressive liver disease leading to cirrhosis and HCC development.

Acknowledgement: We thank Drs. O. M. Andrisani, H. Cho, E. Lara-Pezzi , M. Levrero, S. Murakami, K. I. Nakayama, B. L. Slagle, and J. R. Wands for providing critical reagents and R. López-Rodríguez for statistical analysis.

References

1. Kremsdorf D, Soussan P, Paterlini-Brechot P, Brechot C. Hepatitis B virus-related hepatocellular carcinoma: paradigms for viral-related human carcinogenesis. Oncogene 2006;25:3823-3833.
2. Tang H, Oishi N, Kaneko S, Murakami S. Molecular functions and biological roles of hepatitis B virus x protein. Cancer Sci 2006;97:977-983.
3. Su Q, Schroder CH, Hofmann WJ, Otto G, Pichlmayr R, Bannasch P. Expression of hepatitis B virus X protein in HBV-infected human livers and hepatocellular carcinomas. HEPATOLOGY 1998;27:1109-1120.
4. Park IY, Sohn BH, Yu E, Suh DJ, Chung YH, Lee JH, et al. Aberrant epigenetic modifications in hepatocarcinogenesis induced by hepatitis B virus X protein. Gastroenterology 2007;132:1476-1494.
5. Moon EJ, Jeong CH, Jeong JW, Kim KR, Yu DY, Murakami S, et al. Hepatitis B virus X protein induces angiogenesis by stabilizing hypoxia-inducible factor-1alpha. FASEB J 2004;18:382-384.
6. Kalra N, Kumar V. The X protein of hepatitis B virus binds to the F box protein Skp2 and inhibits the ubiquitination and proteasomal degradation of c-Myc. FEBS Lett 2006;580:431-436.
7. Pei L, Melmed S. Isolation and characterization of a pituitary tumor-transforming gene (PTTG). Mol Endocrinol 1997;11:433-441.
8. Zou H, McGarry TJ, Bernal T, Kirschner MW. Identification of a vertebrate sister-chromatid separation inhibitor involved in transformation and tumorigenesis. Science 1999;285:418-422.
9. Vlotides G, Eigler T, Melmed S. Pituitary tumor-transforming gene: physiology and implications for tumorigenesis. Endocr Rev 2007;28:165-186.
10. Gil-Bernabe AM, Romero F, Limon-Mortes MC, Tortolero M. Protein phosphatase 2A stabilizes human securin, whose phosphorylated forms are degraded via the SCF ubiquitin ligase. Mol Cell Biol 2006;26:4017-4027.
11. Limon-Mortes MC, Mora-Santos M, Espina A, Pintor-Toro JA, Lopez-Roman A, et al. UV-induced degradation of securin is mediated by SKP1-CUL1-beta TrCP E3 ubiquitin ligase. J Cell Sci 2008;121:1825-1831.
12. Ramaswamy S, Ross KN, Lander ES, Golub TR. A molecular signature of metastasis in primary solid tumors. Nat Genet 2003;33:49-54.
13. Fujii T, Nomoto S, Koshikawa K, Yatabe Y, Teshigawara O, Mori T, et al. Overexpression of pituitary tumor transforming gene 1 in HCC is associated with angiogenesis and poor prognosis. HEPATOLOGY 2006;43:1267-1275.
14. Bernal JA, Luna R, Espina A, Lazaro I, Ramos-Morales F, Romero F, et al. Human securin interacts with p53 and modulates p53-mediated transcriptional activity and apoptosis. Nat Genet 2002;32:306-311.
15. Cho-Rok J, Yoo J, Jang YJ, Kim S, Chu IS, Yeom YI, et al. Adenovirus-mediated transfer of siRNA against PTTG1 inhibits liver cancer cell growth in vitro and in vivo. HEPATOLOGY 2006;43:1042-1052.
16. Koike K, Moriya K, Iino S, Yotsuyanagi H, Endo Y, Miyamura T, et al. High-level expression of hepatitis B virus HBx gene and hepatocarcinogenesis in transgenic mice. HEPATOLOGY 1994;19:810-819.
17. Lee S, Tarn C, Wang WH, Chen S, Hullinger RL, Andrisani OM. Hepatitis B virus X protein differentially regulates cell cycle progression in X-transforming versus nontransforming hepatocyte (AML12) cell lines. J Biol Chem 2002;277:8730-8740.

18. Yun C, Cho H, Kim SJ, Lee JH, Park SY, Chan GK. Mitotic aberration coupled with centrosome amplification is induced by hepatitis B virus X oncoprotein via the Ras-mitogen-activated protein/extracellular signal-regulated kinase-mitogen-activated protein pathway. Mol Cancer Res 2004;2:159-169.
19. Benedicto I, Molina-Jimenez F, Bartosch B, Cosset FL, Lavillette D, Prieto J, et al. The tight junction-associated protein occludin is required for a postbinding step in hepatitis C virus entry and infection. J Virol 2009;83: 8012-8020.
20. Ramos-Morales F, Dominguez A, Romero F, Luna R, Multon MC, Pintor-Toro JA, et al. Cell cycle regulated expression and phosphorylation of hpttg proto-oncogene product. Oncogene 2000;19:403-409.
21. Koike K, Moriya K, Yotsuyanagi H, Iino S, Kurokawa K. Induction of cell cycle progression by hepatitis B virus HBx gene expression in quiescent mouse fibroblasts. J Clin Invest 1994;94:44-49.
22. Benn J, Schneider RJ. Hepatitis B virus HBx protein deregulates cell cycle checkpoint controls. Proc Natl Acad Sci U S A 1995;92:11215-11219.
23. Bouchard MJ, Schneider RJ. The enigmatic X gene of hepatitis B virus. J Virol 2004;78:12725-12734.
24. Yun C, Lee JH, Park H, Jin YM, Park S, Park K, et al. Chemotherapeutic drug, adriamycin, restores the function of p53 protein in hepatitis B virus X (HBx) protein-expressing liver cells. Oncogene 2000;19:5163-5172.
25. Lara-Pezzi E, Majano PL, Gomez-Gonzalo M, Garcia-Monzon C, Moreno-Otero R, Levrero M, et al. The hepatitis B virus X protein up-regulates tumor necrosis factor alpha gene expression in hepatocytes. HEPATOLOGY 1998;28:1013-1021.
26. Huang J, Kwong J, Sun EC, Liang TJ. Proteasome complex as a potential cellular target of hepatitis B virus X protein. J Virol 1996;70:5582-5591.
27. Traweger A, Fang D, Liu YC, Stelzhammer W, Krizbai IA, Fresser F, et al. The tight junction-specific protein occludin is a functional target of the E3 ubiquitin-protein ligase itch. J Biol Chem 2002;277:10201-10208.
28. Romero F, Gil-Bernabe AM, Saez C, Japon MA, Pintor-Toro JA, Tortolero M. Securin is a target of the UV response pathway in mammalian cells. Mol Cell Biol 2004;24:2720-2733.
29. Feitelson MA, Reis HM, Liu J, Lian Z, Pan J. Hepatitis B virus X antigen (HBxAg) and cell cycle control in chronic infection and hepatocarcinogenesis. Front Biosci 2005;10:1558-1572.
30. Mukherji A, Janbandhu VC, Kumar V. HBx-dependent cell cycle deregulation involves interaction with cyclin E/A-cdk2 complex and destabilization of p27Kip1. Biochem J 2007;401:247-256.
31. Banks L, Pim D, Thomas M. Viruses and the 26S proteasome: hacking into destruction. Trends Biochem Sci 2003;28:452-459.
32. Frescas D, Pagano M. Deregulated proteolysis by the F-box proteins SKP2 and beta-TrCP: tipping the scales of cancer. Nat Rev Cancer 2008;8:438-449.
33. Mumby M. PP2A: unveiling a reluctant tumor suppressor. Cell 2007;130: 21-24.
34. Christen V, Treves S, Duong FH, Heim MH. Activation of endoplasmic reticulum stress response by hepatitis viruses up-regulates protein phosphatase 2A. HEPATOLOGY 2007;46:558-565.
35. Yu R, Lu W, Chen J, McCabe CJ, Melmed S. Overexpressed pituitary tumor-transforming gene causes aneuploidy in live human cells. Endocrinology 2003;144:4991-4998.
36. Kim CM, Koike K, Saito I, Miyamura T, Jay G. HBx gene of hepatitis B virus induces liver cancer in transgenic mice. Nature 1991;351:317-320.
37. Livezey KW, Negorev D, Simon D. Increased chromosomal alterations and micronuclei formation in human hepatoma HepG2 cells transfected with the hepatitis B virus HBX gene. Mutat Res 2002;505:63-74.
38. Kim S, Park SY, Yong H, Famulski JK, Chae S, Lee JH, et al. HBV X protein targets hBubR1, which induces dysregulation of the mitotic checkpoint. Oncogene 2008;27:3457-3464.

Virology 410 (2011) 38–47

Contents lists available at ScienceDirect

Virology

journal homepage: www.elsevier.com/locate/yviro

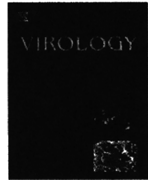

Chaperonin TRiC/CCT participates in replication of hepatitis C virus genome via interaction with the viral NS5B protein

Yasushi Inoue [a,b,c], Hideki Aizaki [a], Hiromichi Hara [a], Mami Matsuda [a], Tomomi Ando [a], Tetsu Shimoji [a], Kyoko Murakami [a], Takahiro Masaki [a], Ikuo Shoji [d], Sakae Homma [b], Yoshiharu Matsuura [e], Tatsuo Miyamura [a], Takaji Wakita [a], Tetsuro Suzuki [a,f,*]

[a] Department of Virology II, National Institute of Infectious Diseases, Tokyo 162-8640, Japan
[b] Department of Respiratory Medicine, Toho University School of Medicine, Tokyo 143-8541, Japan
[c] International University of Health and Welfare, Mita Hospital, Tokyo 108-8329, Japan
[d] Division of Microbiology, Kobe University Graduate School of Medicine, Hyogo 650-0017, Japan
[e] Research Institute for Microbial Diseases, Osaka University, Osaka 565-0871, Japan
[f] Department of Infectious Diseases, Hamamatsu University School of Medicine, Hamamatsu 431-3192, Japan

ARTICLE INFO

Article history:
Received 12 June 2010
Returned to author for revision 18 July 2010
Accepted 15 October 2010
Available online 18 November 2010

Keywords:
Hepatitis C virus
Replication
Non-structural protein
Chaperonin

ABSTRACT

To identify the host factors implicated in the regulation of hepatitis C virus (HCV) genome replication, we performed comparative proteome analyses of HCV replication complex (RC)-rich membrane fractions prepared from cells harboring genome-length bicistronic HCV RNA at the exponential and stationary growth phases. We found that the eukaryotic chaperonin T-complex polypeptide 1 (TCP1)-ring complex/chaperonin-containing TCP1 (TRiC/CCT) plays a role in the replication possibly through an interaction between subunit CCT5 and the viral RNA polymerase NS5B. siRNA-mediated knockdown of CCT5 suppressed RNA replication and production of the infectious virus. Gain-of-function activity was shown following co-transfection with whole eight TRiC/CCT subunits. HCV RNA synthesis was inhibited by an anti-CCT5 antibody in a cell-free assay. These suggest that recruitment of the chaperonin by the viral nonstructural proteins to the RC, which potentially facilitate folding of the RC component(s) into the mature active form, may be important for efficient replication of the HCV genome.

© 2010 Elsevier Inc. All rights reserved.

Introduction

Hepatitis C virus (HCV) is a major cause of chronic liver diseases, such as chronic hepatitis, hepatic steatosis, cirrhosis, and hepatocellular carcinoma (Hoofnagle, 2002; Manns et al., 2006; Saito et al., 1990; Seeff and Hoofnagle, 2003). HCV is an enveloped positive-strand RNA virus belonging to the *Hepacivirus* genus of the Flaviviridae family. Its genome of ~9.6 kb encodes a polyprotein precursor of ~3000 amino acids (aa) (Suzuki et al., 2007; Taguwa et al., 2008). The precursor polyprotein is post- or cotranslationally processed by both viral and host proteases into at least ten viral products. The nonstructural (NS) proteins NS3–NS5B are necessary and sufficient for autonomous HCV RNA replication. They form a membrane-associated replication complex (RC), in which NS5B is the RNA-dependent RNA polymerase (RdRp) that is responsible for copying the RNA genome of the virus during replication. The HCV RC has been detected in detergent-resistant membrane (DRM) structures, possibly in a lipid-raft structure (Aizaki et al., 2004; Shi et al., 2003). Cell-free RC replication activity has also been demonstrated in crude membrane fractions of HCV subgenomic replicon cells (Aizaki et al., 2004; Ali et al., 2002; Hara et al., 2009; Hardy et al., 2003; Yang et al., 2004); these cell-free systems provide semi-intact RdRp assays for biochemical dissection of viral replication.

In general, any process that occurs during viral replication is dependent on the host cell machinery and requires close interaction between viral and cellular proteins. Although evidence that host cell factors interact with HCV NS proteins and are involved in viral replication is accumulating (Moriishi and Matsuura, 2007), the cellular components of HCV RC and their functional roles in viral replication are not fully understood.

Recently, using comparative proteome analysis, we identified 27 cellular proteins that were highly enriched in the DRM fraction of HCV replicon cells relative to parental cells. Subsequent analyses demonstrated that one of the identified proteins, creatine kinase B, a key ATP-generating enzyme, is important for efficient replication of the HCV genome and for production of the infectious virus (Hara et al., 2009).

In this study, to extend our investigation and to increase our understanding of the precise components of HCV RC and the

* Corresponding author. Department of Infectious Diseases, Hamamatsu University School of Medicine, Hamamatsu 431-3192, Japan. Fax: +81 53 435 2337.
E-mail address: tesuzuki@hama-med.ac.jp (T. Suzuki).

0042-6822/$ – see front matter © 2010 Elsevier Inc. All rights reserved.
doi:10.1016/j.virol.2010.10.026

mechanisms of viral genome replication, we designed another comparative proteomic approach in which cells harboring genome-length bicistronic HCV RNA at the exponential growth phase (showing rapid replication of viral RNA) were compared with cells at the confluent-growth phase (showing poor replication of viral RNA). This strategy revealed that the chaperonin T-complex polypeptide (TCP1)-ring complex/chaperonin-containing TCP1 (TRiC/CCT) participates in HCV RNA replication and virion production possibly through an interaction between CCT5 (chaperonin-containing TCP1, subunit 5) and NS5B.

Results

CCT5 and Hsc70 are enriched in the DRM fraction containing the HCV RC

Recently, we analyzed the protein content of DRM fractions prepared from HCV subgenomic replicons and parental Huh-7 cells and identified 27 cellular proteins that were enriched in the DRM fraction prepared from the replicon cells (Hara et al., 2009). These were identified as factors that may be involved in the HCV RC and in viral replication. In fact, subsequent silencing of several genes coding for these proteins resulted in the inhibition of HCV RNA replication (Hara et al., 2009). However, it is likely that proteins unrelated to HCV replication are also included in the identified groups because long-term culture of the replicon cells under the selective pressure of G418 selects for a subpopulation of the parental cells and may induce changes in their protein expression profiles. Thus, to minimize interline differences in culture background, we further designed a comparative proteome analysis using a single cell line as follows.

HCV replication efficiency is dependent on the conditions of host cell growth. High cell density of the replicon culture has a reversible inhibitory effect on viral replication (Nelson and Tang, 2006; Pietschmann et al., 2001). Fig. 1A demonstrates that a high level of HCV RNA was detected in cells harboring the genome-length bicistronic HCV RNA, Con1 strain of genotype 1b (RCYM1) in the growth phase, whereas the RNA level declined sharply when the cells reached the stationary phase. We further compared the synthesis of HCV RNA in cell-free reaction mixtures containing the viral RC isolated from the RCYM1 cells at various cell densities (Fig. 1B). Replication activity was highest at the mid-log phase of cell growth (day 4 after seeding). By contrast, little or no RNA synthesis was observed under the confluent-growth cell culture (day 8), confirming the critical role of host cell growth conditions in the replication of the HCV genome.

Thus, to identify the host cell proteins required for HCV replication, we designed a two-dimensional fluorescence difference gel electrophoresis (2D-DIGE)-based comparative proteomics analysis of RC-rich DRM fractions prepared from RCYM1 cells at the mid-log and confluent-growth phases. Protein spots that reproducibly showed a greater than 1.5-fold difference in the mid-log growth- and the confluent phases were excised and digested by trypsin or lysylendopeptidase. Matrix-assisted laser desorption ionization–time-of-flight (MALDI-TOF) mass spectrometry (MS), which allows identification of the corresponding proteins in 9 cases (Table 1). Two increased spots that showed an increase in levels (their stereoscopic images are shown in Fig. 2A) were identified as CCT5 and Hsc70. CCT5, an epsilon subunit of chaperonin TRiC/CCT, is a 900-kDa toroid-shaped complex consisting of eight different subunits (Valpuesta et al., 2002; Yaffe et al., 1992). Hsc70, a member of the HSP70 family, is a 71-kDa heat shock cognate protein (Dworniczak and Mirault, 1987). Independent of the proteome analyses, DRM fractions and whole cell lysates were prepared from RCYM1 cells at two different growth phases (as above) and were analyzed by immunoblotting (Fig. 2B). Steady-state levels of CCT5 and Hsc70 were obviously higher in the DRM fraction prepared from the cells that were at the mid-log growth phase compared with those at the confluent phase. However, in the whole cell analyses, they were shown to be present at comparable levels during the two different growth phases. These results suggest that expression of CCT5 and Hsc70 is not enhanced in proliferating cells and that the enrichment of these proteins in the DRM fraction is possibly due to their post-translational modification. It should be noted that in the previous proteome analysis, CCT5 and other TRiC/CCT subunits, such as CCT1 and CCT2, were identified as proteins that were enriched in the DRM fraction prepared from subgenomic replicon-containing cells compared with that prepared from parental cells (Hara et al., 2009). We showed that CCT5 and CCT1 were enriched in the DRM fractions of cells transfected with the HCV genomic RNA derived from JFH-1 isolate as well as of subgenomic replicon cells (Fig. 2C).

TRiC/CCT participates in replication of the HCV genome

We investigated gain- and loss-of-functions of TRiC/CCT and Hsc70 with respect to the replication of HCV RNA. Seventy-two hours after RCYM1 cells were transfected with eight plasmids corresponding to each of the TRiC/CCT subunits, the level of HCV RNA in the cells (determined by quantitative RT-PCR) significantly increased to 2-fold that observed in the control cells. However, exogenous expression of Hsc70 in the RCYM1 cells showed no effect on the viral RNA (Fig. 3A). siRNAs targeted to CCT5 or Hsc70 and consisting of pools of three target-specific siRNAs or control nonspecific siRNAs were transfected

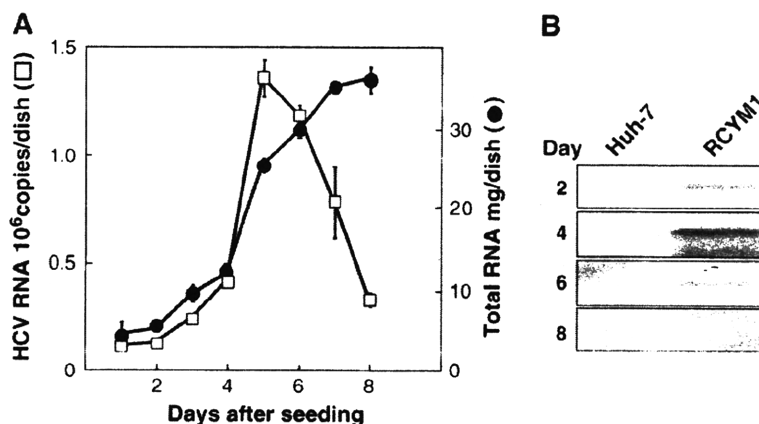

Fig. 1. Effect of cell growth on HCV RNA replication. (A) Measurement of HCV RNA (open squares) and total cellular RNA (closed circles) in RCYM1 cells at the time of harvest (days after seeding). (B) DRM fractions obtained from RCYM1 and parental Huh-7 cells harvested as indicated (day) were analyzed by cell-free RNA replication assay. RNA extracted from each sample was analyzed by agarose gel electrophoresis and autoradiograph.

Table 1
Selected cellular proteins that reproducibly increased and decreased in membrane fraction of RCYM1 cells at exponential growth phase.

Av. ratio	T-test	Coverage (%)	Protein name	Molecular function	GI
Increased proteins					
1.58	0.017	31	CCT5	Protein folding	33879913
1.54	0.005	35	HSPA8 (Hsc70)	Protein folding	24657660
Decreased proteins					
−1.95	0.028	44	Creatine kinase isozyme CK-B gene, exon 8	Energy pathway/metabolism	180568
−1.53	0.011	16	Chain C, Human Sirt2 Histone deacetylase	Cell cycle control	15826438
−2.14	0.001	33	Proteasome regulatory particle subunit p44S10	Metabolism	15341748
−1.71	0.004	21	Aldehyde dehydrogenase	Metabolism	178388
−1.85	0.004	40	Aminoacylase 1	Metabolism	12804328
−2.77	0.003	15	Eukaryotic translation initiation factor 3, subunit 3 gamma	Metabolism (translation regulator activity)	6685512
−2.43	0.014	20	Intraflagellar transport protein 74 homolog (Coiled-coil domain-containing protein 2)	Cell growth and/or maintenance	10439078

Three paired samples of RC-rich membrane fractions at the exponential- and confluent-growth phases of RCYM1 cultures were analyzed. The proteins representing a more than 1.5-fold increase or decrease (−) reproducibly and significantly are indicated.
Coverage (%): the ratio of the portion of protein sequence covered by matched peptides to the whole sequence.
GI: GenInfo Identifier number.

into RCYM1 cells. After 72 h, the HCV RNA level was reduced by 42% and 27% in the cells transfected with siRNAs against CCT5 and Hsc70, respectively, compared with controls (Fig. 3B). TRiC/CCT possibly interacts with Hsc70, and its complex formation contributes to increasing the efficiency of protein folding (Cuéllar et al., 2008). Our results suggest the involvement of TRiC/CCT and Hsc70 in the HCV life cycle. In particular, TRiC/CCT may play an important role in the replication of the viral genome.

To verify the specificity of the knockdown of CCT5 siRNA, we further synthesized two siRNAs targeted to different regions used in the above CCT5 siRNA and assessed their knockdown effect on HCV genome replication (Fig. 3C, upper panel). As expected, transfection of

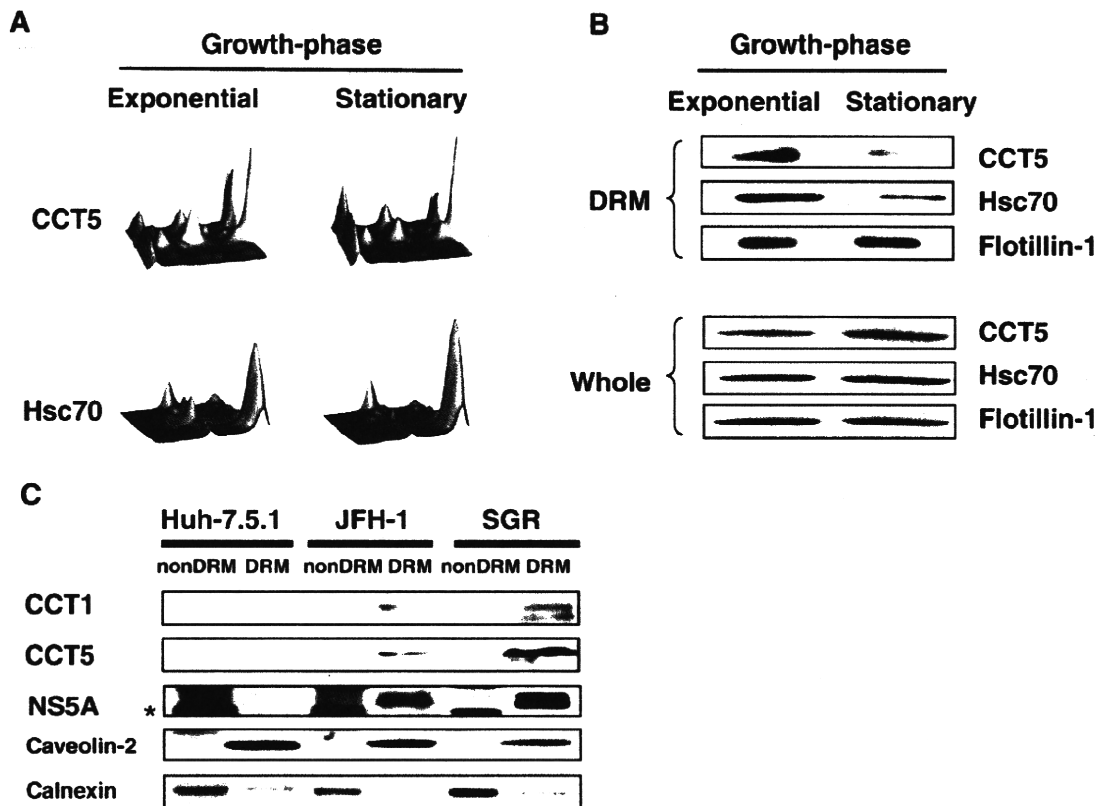

Fig. 2. Comparison of protein levels in DRM fractions prepared from RCYM1 cells at the exponential and stationary growth phases. (A) Three-dimensional images of CCT5 and Hsc70 analyzed by Ettan DIGE (GE Healthcare). Spots corresponding to CCT5/Hsc70 at exponential and stationary growth phases of the cells, respectively, are shown in green and red. (B) Equal amounts of protein in the DRM fractions prepared from RCYM1 cells at the exponential and stationary growth phases or corresponding whole cell lysates were analyzed by immunoblotting with Abs against CCT5, Hsc70 or flotillin-1. (C) Enrichment of CCT1 and CCT5 in the DRM fractions of HCV RNA replicating cells. Equal amounts of DRM or non-DRM fractions from full-length JFH-1 RNA transfected cells (JFH-1), subgenomic replicon cells (SGR) and parental Huh-7.5.1 cells were analyzed by immunoblotting with antibodies against CCT1, CCT5, NS5A, caveolin-2 or calnexin. *Non-specific bands.

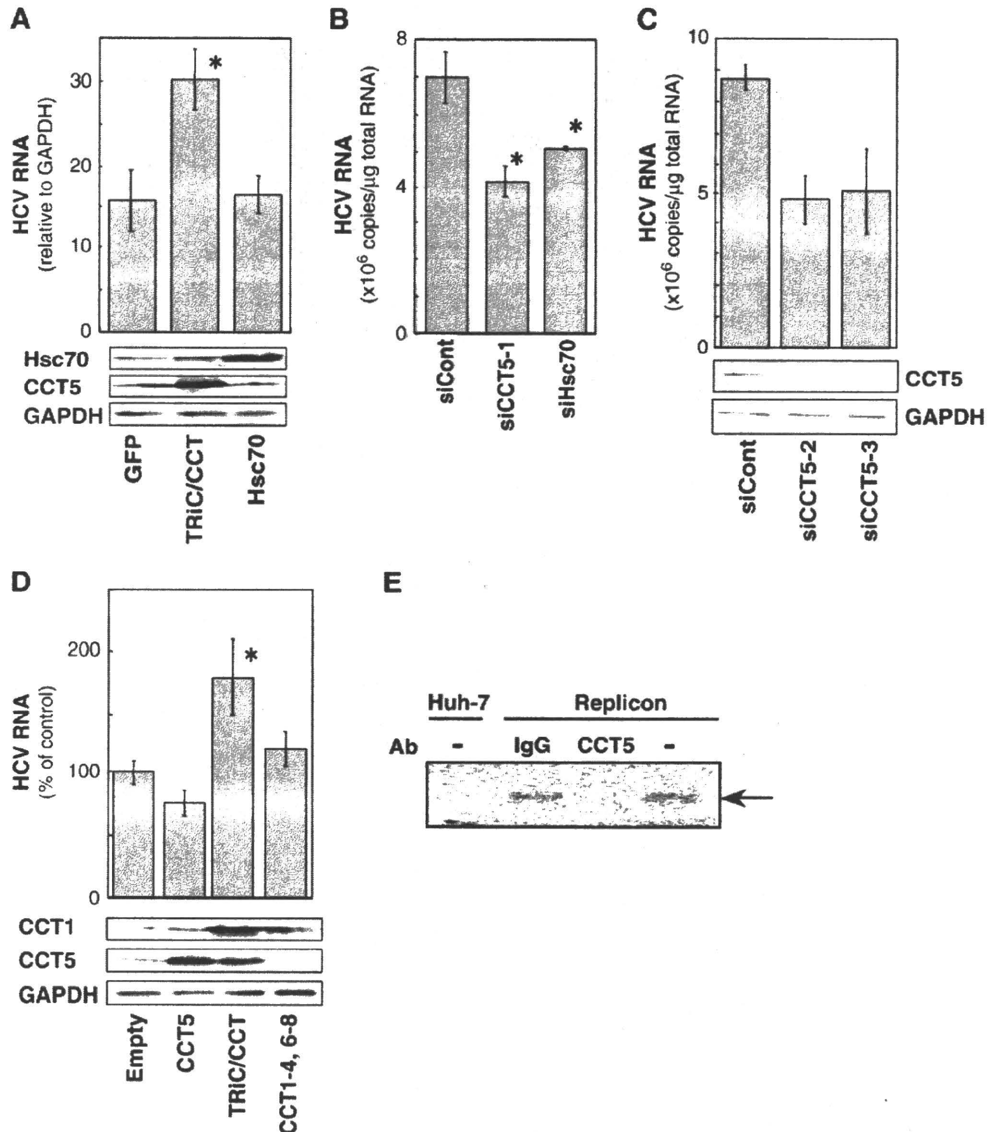

Fig. 3. Involvement of TRiC/CCT in HCV replication (A and D). Overexpression of all eight subunits of TRiC/CCT (TRiC/CCT); seven subunits, CCT1, 2, 3, 4, 6, 7, and 8 (CCT1-4, 6-8); subunit CCT5 only (CCT5); Hsc70; or control GFP in RCYM1 cells. HCV RNA levels were determined 48 h post-transfection (B and C). Knockdown of endogenous CCT5 or Hsc70 in RCYM1 cells, which were transfected with three types of siRNAs against CCT5 (siCCT5-1, -2, and -3), siRNA against Hsc70 (siHsc70), or control siRNA (siCont), and were harvested at 72 h post-transfection. siCCT5-1 and siHsc70 consisted of pools of three target-specific siRNAs. Immunoblotting for CCT1, CCT5, Hsc70 and GAPDH was performed (A, C and D; lower). (E) Cell-free de novo viral RNA synthesis assays were performed in the presence of anti-CCT5 Ab or control mouse IgG. Cytoplasmic fractions from SGR-N (replicon) and parental Huh-7 cells were used. An arrow indicates the synthesized HCV RNA. Error bars denote standard deviations with asterisks indicating statistical significance (*$P<0.01$).

RCYM1 cells with each CCT5 siRNA resulted in a reduction in viral RNA to a level of about 50% of that observed in cells treated with control siRNAs. Immunoblotting confirmed the efficient reduction in expression of endogenous CCT5 and the lack of cytotoxic effect exerted by the CCT5 siRNAs (Fig. 3C, middle and lower panels).

Having confirmed the upregulation of HCV RNA by ectopic expression of all the TRiC/CCT subunits, we further addressed the possibility that CCT5, independent of the complete TRiC/CCT complex, might have a role in promoting replication of HCV RNA. Transfection with either a CCT5 expression plasmid alone or with seven plasmids expressing all the TRiC/CCT subunits except CCT5 resulted in no or only a slight increase in the level of HCV RNA, indicating that all CCT subunits are required for HCV replication (Fig. 3D).

TRiC/CCT is generally known as a cytosolic chaperone (Valpuesta et al., 2002). However, it is enriched in the DRM fraction of HCV-replicating cells during the exponential growth phase (Fig. 2B). We used immunofluorescence staining to investigate whether TRiC/CCT is localized in the intracellular membrane compartments where replication of the viral genome occurs (Fig. 4). The de novo-synthesized RdRp was labeled by bromouridine triphosphate (BrUTP) incorporation in the presence of actinomycin D, and brominated nucleotides were detected with a specific antibody (Ab). Fluorescence staining in distinct speckles of various sizes was found in the cytoplasm of the HCV subgenomic replicon cells, whereas no signal was detected in the control cells, indicating that the observed BrUTP-incorporating RNA is mostly viral, newly synthesized viral RNA (Fig. 4A). Double immunofluorescence staining showed that a certain section of CCT5 co-distributed with the BrUTP-labeled RNA (Fig. 4A), which is known to co-exist with HCV NS proteins in viral replicating cells (Shi et al., 2003). We further observed that CCT5 was at least partially colocalized

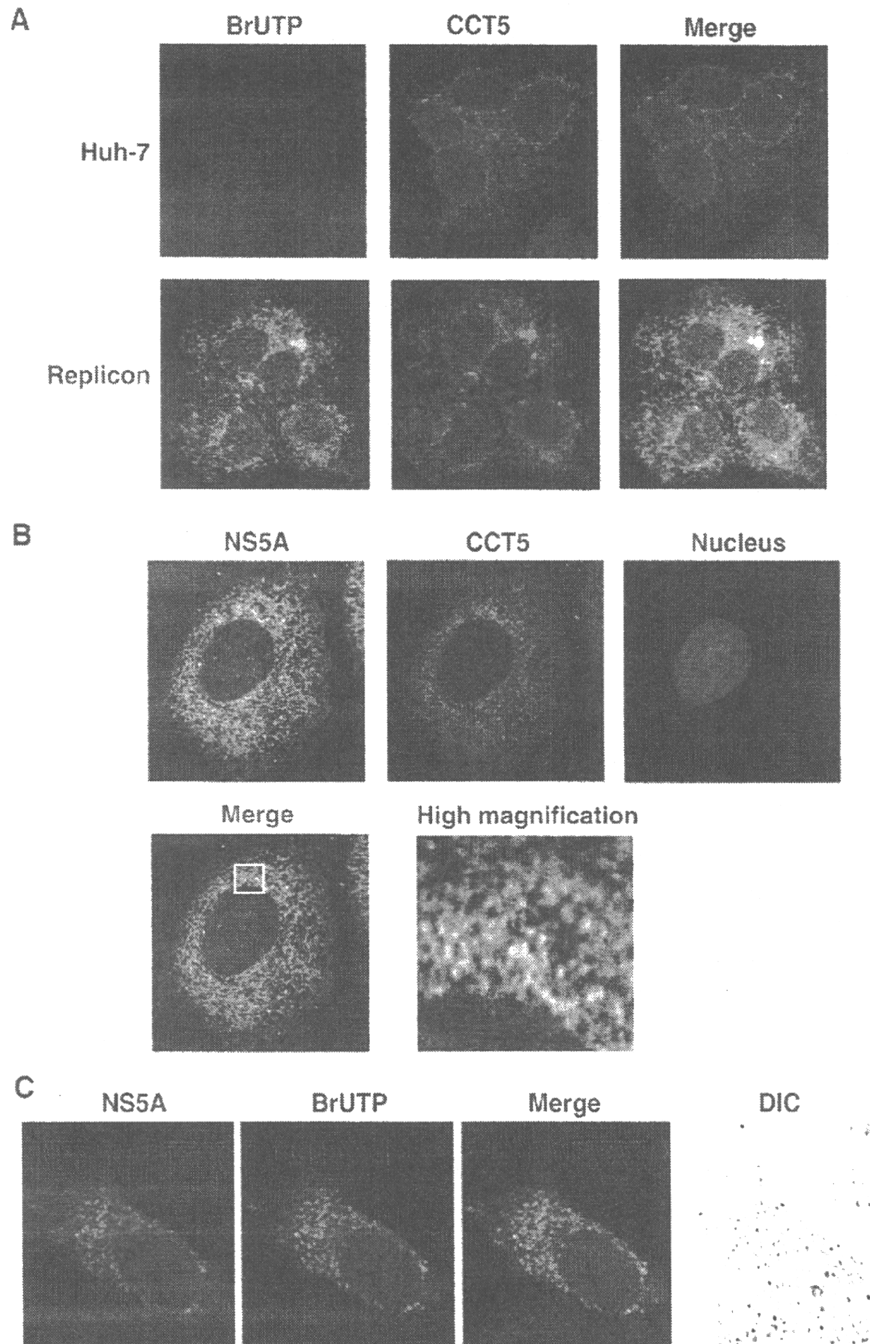

Fig. 4. Immunofluorescence analysis of CCT5 in SGR-N and Huh-7 cells (A) and HCVcc-infected cells (B). The primary Abs used were anti-CCT5 goat polyclonal Ab (red), anti-BrUTP monoclonal Ab (green), and anti-NS5A monoclonal Ab (green). Merged images of red and green signals (A) or of red, green and blue (nucleus) signals (B) are shown. The high magnification panel is an enlarged image of a white square of the merge panel. (C) Colocalization of NS5A protein with the viral RNA. The replicon cells were permeabilized with lysolecithin and labeled with BrUTP, followed by staining with anti-NS5A rabbit polyclonal Ab (red) and the anti-BrUTP monoclonal Ab (green). DIC, differential interference contrast.

with the viral NS protein in certain compartments sharing a dot-like structure in Huh-7 cells infected with HCV JFH-1 infectious HCV (HCVcc) derived from HCV genotype 2a (Fig. 4B) as well as in the replicon cells (data not shown). Fig. 4C indicated co-localization of BrUTP-labeled RNA with NS5A.

To further address the role of TRiC/CCT in HCV genome replication, we performed immunodepletion and in vitro replication analyses, which have been used for studying the genome replication of several viruses (Daikoku et al., 2006; Garcin et al., 1993; Liu et al., 2009). Cell extracts prepared from the HCV-replicating cells were reacted with either a mouse monoclonal Ab against CCT5 or mouse IgG derived from preimmune serum, followed by cell-free synthesis of HCV RNA. Fig. 3E shows that treatment with anti-CCT5 Ab inhibited viral RNA synthesis, whereas the control IgG did not affect the process, suggesting that TRiC/CCT participates directly in HCV RNA replication.

CCT5 interacts with HCV NS5B

The genome replication machinery of HCV is a membrane-associated complex composed of multiple factors including viral NS proteins. Given the involvement of TRiC/CCT in HCV RNA synthesis, we next examined its possible interaction with HCV NS proteins. A first attempt to immunoprecipitate the viral proteins with antibodies against TRiC/CCT subunits in the replicon cells was unsuccessful (data not shown), suggesting that endogenous levels of TRiC/CCT is not sufficient to pull out NS5B. Next, dual (myc/FLAG)-tagged NS3, NS5A, or NS5B proteins derived from the genotype 1b NIHJ1 strain were co-expressed with CCT5 in Huh-7 cells and then subjected to two-step immunoprecipitation with anti-myc and anti-FLAG Abs (Ichimura et al., 2005; Shirakura et al., 2007). An empty plasmid was used as a negative control in the analyses. As shown in Fig. 5A, CCT5 specifically interacted with NS5B. Little or no interaction was found between CCT5 and NS3 or NS5A. To determine the NS5B region required for the interaction with CCT5, various deletion mutants of HA-NS5B were constructed and their interactions with CCT5 were analyzed as described above. CCT5 was shown to be coimmunoprecipitated with either a full-length NS5B (aa 1–591), an N-terminal deletion (aa 71–591) or a C-terminal deletion (aa 1–570), but not with deletions aa 215–591 or aa 320–591 (Fig. 5B), suggesting that aa 71–214 of NS5B are important for its interaction with CCT5.

Knockdown of CCT5 results in the reduction of propagation of infectious HCV

We further examined whether the knockdown of CCT5 would abrogate the production of infectious HCV (HCVcc), derived from JFH-1 (Fig. 6). At 72 h post-transfection with each CCT5 siRNA, HCV RNA levels in Huh-7 cells infected with HCVcc were reduced by 25–35% compared with controls. Accordingly, virion production from CCT5 siRNA-transfected cultures was significantly decreased, as determined by intracellular HCV core protein levels at 72 h after the infection of naïve cells with culture supernatants taken from transfected cells. These results demonstrate that reduction of the HCV RNA replication by siRNA-mediated knockdown of CCT5 results in reduction of the propagation of the infectious virus.

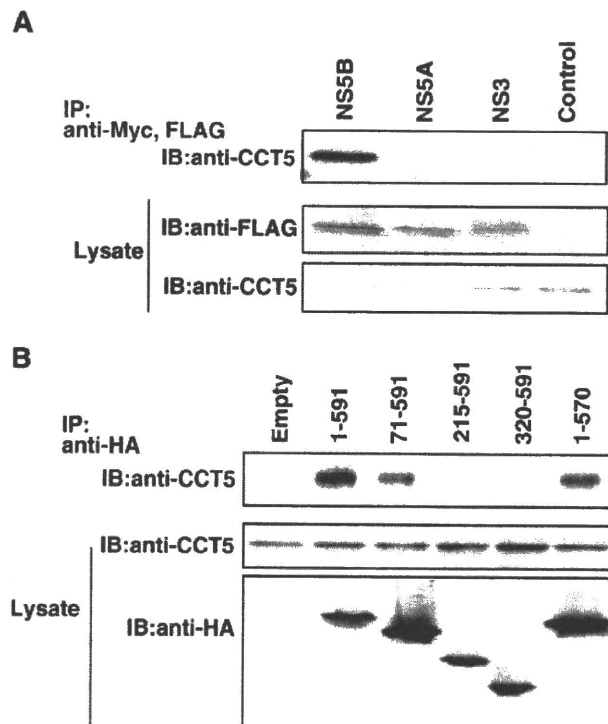

Fig. 5. CCT5 interacts with HCV NS5B. (A) CCT5 was co-expressed with MEF-tagged-NS5B, -NS5A, or -NS3 protein of strain NIHJ1 in cells, followed by two-step immunoprecipitation (IP) with anti-FLAG and anti-myc Abs. Immunoprecipitates were subjected to immunoblotting with anti-CCT5 Ab (IB). (B) Full-length NS5B (1–591) or its deletions (71–591, 215–591, 320–591, 1–570) along with a HA tag were co-expressed with CCT5. IP and IB were performed as described above.

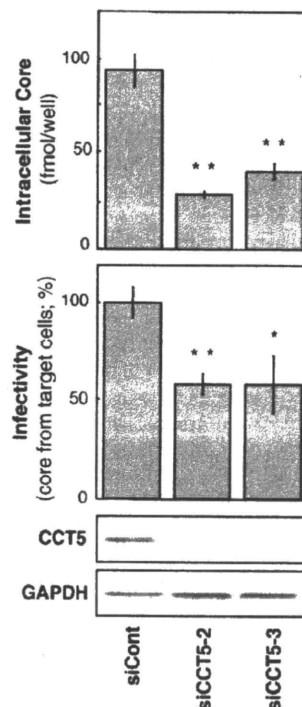

Fig. 6. Knockdown of endogenous CCT5 in HCVcc-infected cells. The cells were transfected with siRNAs against CCT5 (siCCT5-2, -3) or with control siRNAs (siCont). At 72 h post-transfection, the viral core protein levels in cells were determined (upper panel). Collected culture supernatants were inoculated into naïve Huh7.5.1 cells and intracellular core proteins were determined at 72 h post-infection (middle panel). Cells transfected with siRNAs were analyzed by immunoblotting with anti-CCT5 or anti-GAPDH Ab (lower panel). Error bars denote standard deviations with asterisks indicating statistical significance (*$P<0.05$; **$P<0.01$).

Discussion

The chaperone-assisted protein-folding pathway is a process in living cells that results from coordinated interactions between multiple proteins that often form multi-component complexes. Several steps in the viral life cycle, such as protein processing, genome replication, and viral assembly, are regulated by cellular chaperones. Hsp90, one of the most abundant proteins in unstressed cells, has been implicated in HCV RNA replication (Nakagawa et al., 2007; Okamoto et al., 2006, 2008; Taguwa et al., 2008, 2009; Ujino et al., 2009). FKBP8, a member of the FKBP506-binding protein family, and hB-ind1, human butyrate-induced transcript 1, play key roles through their interaction with HCV NS5A and Hsp90 (Okamoto et al., 2006, 2008; Taguwa et al., 2008, 2009). Hsp90 has also been implicated in viral enzymatic activities including those of the influenza virus (Momose et al., 2002; Naito et al., 2007), herpes simplex virus (Burch and Weller, 2005), Flock house virus (Kampmueller and Miller, 2005), and hepatitis B virus (Hu et al., 2004).

In our former study, comparative proteome analyses of the viral RC-rich DRM fractions prepared from subgenomic replicon cells and Huh-7 cells were carried out to identify host factors involved

in HCV replication (Hara et al., 2009). We extended the proteomics by modifying our protocol of the analysis to reduce the interline differences in culture background and analyzed the DRM samples derived from the mid-log and confluent-growth phases of single cell line. Here, we identified two proteins, CCT5 and Hsc70, showing an increase in levels at the mid-log growth phase. Although CCT5 was also identified in the former study as expected, Hsc70 was not included in the list of proteins identified in the study (Hara et al., 2009). This difference may be due to the use of cells carrying the full-length replicon RNA in this study.

In this study, we demonstrated that TRiC/CCT participates in HCV RNA replication and virion production possibly through its interaction with NS5B. TRiC/CCT is a group II chaperonin that assists in protein folding in eukaryotic cells and forms a double-ring-like hexadecamer complex. Although relatively little is known about its function compared with that of the group I chaperonins such as bacterial GroEL, several mammalian proteins whose folding is mediated by TRiC/CCT have been identified, such as actin, tubulin, and von Hippel–Lindau tumor suppressor protein (Farr et al., 1997; Feldman et al., 2003; Frydman and Hartl, 1996; Meyer et al., 2003; Tian et al., 1995). With regard to viral proteins, the Epstein–Barr virus nuclear antigen, HBV capsid protein, and p4 of M-PMV have been identified as TRiC/CCT-interacting proteins (Yam et al., 2008). However, the functional significance of their interactions in the viral life cycles has yet to be determined. Here we demonstrated that the reduction in CCT5 expression in HCV replicon cells and in virus-infected cells inhibits HCV RNA replication (Figs. 3B and C) and virus production (Fig. 6) respectively. Gain-of-function was also shown by co-transfection of the replicon cells with eight constructs corresponding to all the TRiC/CCT subunits (Figs. 3A and D).

A recent study of the three-dimensional structure of the TRiC/CCT and Hsc70 complex has demonstrated that the apical domain of the CCT2 (CCT-beta) subunit is involved in the interaction with Hsc70 (Cuéllar et al., 2008). The complex formation created by the TRiC/CCT and Hsc70 interaction may promote higher efficiency in the folding of certain proteins (Cuéllar et al., 2008). In our comparative proteome analyses, both CCT subunits and Hsc70 were enriched in the HCV RC-rich membrane fraction of the replicon cells that showed high viral replication activity (Fig. 2B). Transfection of Hsc70 siRNA into the replicon cells moderately inhibited viral RNA replication (Fig. 3B). However, upregulation of HCV replication was not observed by ectopic expression of Hsc70 (Fig. 3A), and little or no interaction was observed between Hsc70 and HCV NS proteins in the co-immunoprecipitation analysis (data not shown). Thus, it is likely that TRiC/CCT acts as a regulator of HCV replication through participating in the de novo folding of NS5B RdRp, and Hsc70 might serve to assist in folding through its interaction with TRiC/CCT. It was recently reported that Hsc70 is associated with HCV particles and modulates the viral infectivity (Parent et al., 2009). Here we showed an additional role of Hsc70 in the HCV life cycle.

HCV genomic single-stranded RNA serves as a template for the synthesis of the full-length minus strand that is used for the overproduction of the virus-specific genomic RNA. NS5B RdRp is a single subunit catalytic component of the viral replication machinery responsible for both of these processes. It is known that the in vitro RdRp activity of recombinant NS5B expressed in and purified from insect cells and *Escherichia coli* is low in many cases. This could be due to the lack of a suitable cellular environment for favorable RdRp activity, although the particular conformational features dependent on the viral isolates may also be involved (Lohmann et al., 1997; Weng et al., 2009). In fact, besides interacting with HCV NS proteins, NS5B has been reported to interact with several host cell proteins. For example, human vesicle-associated membrane protein-associated protein subtype A (VAP-A) and subtype B (VAP-B), which are involved in the regulation of membrane trafficking, lipid transport and metabolism, and the unfolded protein response, interact with NS5B and NS5A and participate in HCV replication (Hamamoto et al., 2005). Recently, VAP-C, a splicing variant of VAP-B, was found to act as a negative regulator of viral replication through its interaction with NS5B but not with VAP-A (Kukihara et al., 2009). Cyclophilin A and B, peptidyl-prolyl isomerases that facilitate protein folding by catalyzing the *cis–trans* interconversion of peptide bonds at proline residues, play a role in stimulating HCV RNA synthesis through interaction with NS5B (Liu et al., 2009; Watashi et al., 2005). SNARE-like protein (Tu et al., 1999), eIF4AII (Kyono et al., 2002), protein kinase C-related kinase 2 (Kim et al., 2004), nucleolin (Kim et al., 2004; Hirano et al., 2003; Shimakami et al., 2006), and p68 (Goh et al., 2004) are also known to associate with NS5B and are possibly involved in HCV RNA replication.

We found that the aa 71–214 region in NS5B is important for interaction with TRiC/CCT. The catalytic domain of HCV RdRp has a "right-hand" configuration similar to other viral polymerases, such as HIV-1 reverse transcriptase (Huang et al., 1998) and poliovirus RdRp (Hansen et al., 1997), and is divided into the fingers, palm, and thumb functional subdomains (Lohmann et al., 2000). The region required for the interaction with TRiC/CCT has been mapped in a part of the fingers and palm domains of NS5B RdRp. To address how TRiC/CCT assists in the correct folding or disaggregation of NS5B through their interaction, leading to the formation of a functional RdRp, work based on an in vitro reconstitution system using purified proteins is under way. As all the TRiC/CCT subunits possess essentially identical ATPase domains, their protein-recognition regions are apparently divergent, allowing for substrate-binding specificity. It has recently been reported that TRiC/CCT interacts with the PB2 subunit of the influenza virus RNA polymerase complex and TRiC/CCT binding site is located in the central region of PB2, suggesting involvement of TRiC/CCT in the influenza virus life cycle (Fislová et al., 2010). Eukaryotic RNA polymerase subunit has also been identified as a binding partner of TRiC/CCT from interactome analysis (Yam et al., 2008). It would be interesting to examine how conserved the mechanisms of TRiC/CCT action that result in enhanced replication are among RNA polymerases.

The recruitment of a chaperonin by viral NS proteins may be important for understanding regulation of the viral genome replication. In this study, we demonstrated the involvement of TRiC/CCT in HCV RNA replication possibly through its interaction between TRiC/CCT and HCV NS5B. Although possible interaction of subunit CCT5 with NS5B was shown, considering involvement of whole TRiC/CCT complex in its chaperonin function, whether CCT5 directly interacts with NS5B is unclear. Further detailed studies are needed to make clear the manner of TRiC/CCT-NS5B interaction. NS5B RdRp is one of the main targets for HCV drug discovery. The search for NS5B inhibitors has resulted in the identification of several binding sites on NS5B, such as the domain adjacent to the active site and the allosteric GTP site (De Francesco and Migliaccio, 2005; Laporte et al., 2008). The findings obtained here suggest that disturbing the interaction between NS5B and TRiC/CCT may be a novel approach for an antiviral chemotherapeutic strategy.

Materials and methods

Cell culture, transfection, and infection

Human hepatoma Huh-7 and Huh-7.5.1 cells (kindly provided by Francis V. Chisari from The Scripps Research Institute) and human embryonic kidney 293T cells were maintained in Dulbecco's modified Eagle's medium (DMEM) supplemented with 10% fetal calf serum. Huh-7-derived SGR-N (Shi et al., 2003) and RCYM1 (Murakami et al., 2006) cells, which possess subgenomic replicon RNA from the HCV-N strain (Guo et al., 2001; Ikeda et al., 2002) and genome-length HCV RNA from the Con 1 strain (Pietschmann et al., 2002), were cultured in the above medium in the presence of 1 mg/ml G418. Cells were transfected with plasmid DNAs using FuGENE transfection reagents

(Roche Diagnostics, Tokyo, Japan). Culture media from Huh-7 cells transfected with in vitro-transcribed RNA corresponding to the full-length HCV RNA derived from the JFH-1 strain (Wakita et al., 2005) were collected, concentrated, and used for the infection assay (Aizaki et al., 2008).

Ab

Primary Abs used in this study were mouse monoclonal Abs against FLAG (Sigma-Aldrich, St. Louis, MO), c-myc (Sigma-Aldrich), CCT5 (Abnova Corporation, Taipei City, Taiwan), flotillin-1 (BD Biosciences, San Jose, CA), glyceraldehyde-3-phosphate dehydrogenase (GAPDH) (Chemicon, Temecula, CA), BrdU (Caltag, CA) and HCV NS5A (Austral Biologicals, San Ramon, CA), a rabbit polyclonal Ab against hemagglutinin (HA; Sigma-Aldrich), a sheep polyclonal Ab against bromodeoxyuridine (Biodesign International, Saco, ME), and goat polyclonal Abs against the individual subunits of CCT (Santa Cruz Biotechnology, Santa Cruz, CA) and Hsc70 (Santa Cruz Biotechnology). Anti Hsc70 and CCT5 monoclonal rat Abs were obtained from Abcam (Tokyo, Japan) and AbD serotec (Oxford, UK). Rabbit polyclonal antibody to NS5A was described previously (Hamamoto et al., 2005). Anti NS5B monoclonal Ab was kindly provided by D. Moradpour (Centre Hospitalier Universitaire Vaudois, University of Lausanne; Moradpour et al., 2002).

Plasmids

To generate expression plasmids for the NS proteins with dual epitope tags, DNA fragments encoding the NS3, NS5A, or NS5B proteins were amplified from HCV strain NIHJ1 (Aizaki et al., 1998) by PCR and cloned into the EcoRI–EcoRV sites of pcDNA3-MEF, which includes the MEF tag cassette containing the *myc* tag, TEV protease cleavage site, and FLAG tag sequences (Ichimura et al., 2005; Shirakura et al., 2007). To create a series of NS5B truncation mutants, each fragment was amplified by PCR and cloned into the EcoRI–XhoI site of pCMV-HA (Clontech, Mountain View, CA). To generate expression plasmids for the individual CCT subunits, cDNA fragments encoding human CCT1 through CCT8 were amplified from the total cellular RNA by RT-PCR and then cloned into the SmaI site of pCAGGS (Niwa et al., 1991). All PCR products were confirmed by nucleotide sequencing.

Proteome analysis

RC-rich membrane fractions from the cells were isolated as described previously (Aizaki et al., 2004). Briefly, cells were lysed in hypotonic buffer. After removing the nuclei, the supernatants were mixed with 70% sucrose, overlaid with 55% and 10% sucrose, and centrifuged at 38,000 rpm for 14 h. Proteins from the membrane fractions were then analyzed by 2D-DIGE as described previously (Hara et al., 2009). Briefly, protein samples were resolved in protein solubilization buffer (Bio-Rad Laboratories, Tokyo, Japan) and washed with pH adjustment buffer (7 M urea, 2 M thiourea, 4% CHAPS, 30 mM Tris–HCl [pH 10.0]), before being labeled with fluorescent dyes; the dyes used were Cy3 for RCYM1 cells samples taken at the exponential growth phase, Cy5 for cells samples taken at the confluent phase, and Cy2 for a protein standard containing equal amounts of both cell samples. Aliquots of the labeled samples were pooled and applied to Immobiline DryStrip (GE Healthcare, Tokyo, Japan) for first-dimension separation and to 12.5% polyacrylamide gels for second-dimension separation. Images of the 2-D gels were captured on a Typhoon scanner (GE Healthcare), and analyzed quantitatively using DeCyder v5.0 software (GE Healthcare). Samples were analyzed in triplicate as independent cultures and the Student's *t*-test was applied using the DeCyder biological variation analysis module to validate the significance of the differences in spot intensity detected between the samples.

In vitro RNA replication assay

In vitro replication of HCV RNA was performed as described previously (Hamamoto et al., 2005). Briefly, cytoplasmic fractions of subgenomic replicon cells were treated with 1% NP-40 at 4 °C for 1 h, followed by being incubated with 1 mM of ATP, GTP, and UTP; 10 μM CTP; [^{32}P]CTP (1 MBq; 15 TBq/mmol); 10 μg/ml actinomycin D; and 800 U/ml RNase inhibitor (Promega, Madison, WI) for 4 h at 30 °C. RNA was extracted from the total mixture by using TRI Reagent (Molecular Research Center, Cincinnati, OH). The RNA was precipitated, eluted in 10 μl of RNase-free water, and analyzed by 1% formaldehyde-agarose gel electrophoresis. For the immunodepletion assay, the cytoplasmic fractions were incubated with anti-CCT5 Ab in the presence of NP-40 for 4 h before NTP incorporation.

MALDI-TOF MS analysis

Target spots were cut and collected from gels under UV luminescence and rechecked with Typhoon scanner. The spot gels of the target proteins were subjected to in-gel trypsin digestion and analyzed by MALDI-TOF MS meter (Voyager-DE STR, Applied Biosystems, Tokyo, Japan) as described previously (Yanagida et al., 2000). All proteins were identified by peptide mass fingerprinting.

Immunoblot analysis and immunoprecipitation

Immunoblot analysis was performed essentially as described previously (Aizaki et al., 2004). The membrane was visualized with SuperSignal West Pico chemiluminescent substrate (Pierce, Rockford, IL). For immunoprecipitation, cells transfected with plasmids expressing epitope-tagged HCV protein or CCT5 were lysed and then subjected to two-step precipitations with anti-myc and anti-FLAG Abs according to the procedures described previously (Ichimura et al., 2005). In some experiments, HA-tagged full-length NS5B (aa 1–591) or its deletion mutants (aa 71–591, 215–591, 320–591, 1–570) were co-expressed with CCT5 in cells, followed by single-step immunoprecipitation and immunoblotting.

Immunofluorescence staining

Cell permeabilization with lysolecithin and detection of de novo-synthesized viral RNA was performed as described previously (Shi et al., 2003). Briefly, Huh-7 cells were plated on 8-well chamber slides at a density of 5×10^4 cells per well. Cells were incubated with actinomycin D (5 μg/μl) for 1 h and were washed twice with serum-free medium, before being incubated for 10 min on ice. The cells were then incubated in a transcription buffer containing 0.5 mM BrUTP for 30 min. The cells were fixed in 4% formaldehyde for 20 min and then incubated for 15 min in 0.1% Triton X-100 in phosphate-buffered saline (PBS). Primary Abs were diluted in 5% bovine serum albumin in PBS and were incubated with the cells for 1 h. After washing with PBS, fluorescein-conjugated secondary Abs (Jackson Immunoresearch Laboratories, West Grove, PA) were added to the cells at a 1:200 dilution for 1 h. The slides were then washed with PBS and mounted in ProLong Antifade (Molecular Probes, Eugene, OR). Confocal microscopy was performed on a Zeiss Confocal Laser Scanning Microscope LSM 510 (Carl Zeiss MicroImaging, Thornwood, NY).

RNA interference

Small interfering RNAs (siRNAs) targeted to CCT5 or Hsc70 and scrambled negative control siRNAs were purchased from Sigma-Aldrich Japan (Tokyo, Japan). Cells were plated on a 24-well plate with

antibiotic-free DMEM overnight, and each plate was transfected with 10 nM siRNAs by X-tremeGENE (Roche Diagnostics) according to the manufacturer's protocol. Forty-eight hours post-transfection, the total RNA and protein extracts were prepared and subjected to real-time RT-PCR and immunoblot analyses, respectively.

Quantitation of HCV RNA and core protein

Total RNA was extracted from cells using TRIzol reagent (Invitrogen, Carlsbad, CA) according to the manufacturer's instructions. Real-time RT-PCR was performed using TaqMan EZ RT-PCR Core Reagents (PE Applied Biosystems, Foster City, CA) as described previously (Aizaki et al., 2004; Murakami et al., 2006). HCV core protein levels in the cells and in the supernatant were quantified using an HCV core enzyme-linked immunosorbent assay (Ortho-Clinical Diagnostics, Tokyo, Japan).

Acknowledgments

We thank Drs. F. V. Chisari (The Scripps Research Institute) and D. Moradpour (Centre Hospitalier Universitaire Vaudois, University of Lausanne) for providing the Huh-7.5.1 cells and anti-NS5B monoclonal antibody, respectively; S. Yoshizaki, M. Kaga, M. Sasaki, and T. Date for their technical assistance, and T. Mizoguchi for secretarial work. This work was supported by a grant-in-aid for Scientific Research from the Japan Society for the Promotion of Science, from the Ministry of Health, Labour and Welfare of Japan, and from the Ministry of Education, Culture, Sports, Science and Technology, and by Research on Health Sciences focusing on Drug Innovation from the Japan Health Sciences Foundation, and by the Program for Promotion of Fundamental Studies in Health Sciences of the National Institute of Biomedical Innovation of Japan.

References

Aizaki, H., Aoki, Y., Harada, T., Ishii, K., Suzuki, T., Nagamori, S., Toda, G., Matsuura, Y., Miyamura, T., 1998. Full-length complementary DNA of hepatitis C virus genome from an infectious blood sample. Hepatology 27 (2), 621–627.

Aizaki, H., Lee, K.J., Sung, V.M., Ishiko, H., Lai, M.M., 2004. Characterization of the hepatitis C virus RNA replication complex associated with lipid rafts. Virology 324 (2), 450–461.

Aizaki, H., Morikawa, K., Fukasawa, M., Hara, H., Inoue, Y., Tani, H., Saito, K., Nishijima, M., Hanada, K., Matsuura, Y., Lai, M.M., Miyamura, T., Wakita, T., Suzuki, T., 2008. Critical role of virion-associated cholesterol and sphingolipid in hepatitis C virus infection. J. Virol. 82 (12), 5715–5724.

Ali, N., Tardif, K.D., Siddiqui, A., 2002. Cell-free replication of the hepatitis C virus subgenomic replicon. J. Virol. 76 (23), 12001–12007.

Burch, A.D., Weller, S.K., 2005. Herpes simplex virus type 1 DNA polymerase requires the mammalian chaperone hsp90 for proper localization to the nucleus. J. Virol. 79 (16), 10740–10749.

Cuéllar, J., Martín-Benito, J., Scheres, S.H., Sousa, R., Moro, F., López-Viñas, E., Gómez-Puertas, P., Muga, A., Carrascosa, J.L., Valpuesta, J.M., 2008. The structure of CCT-Hsc70 NBD suggests a mechanism for Hsp70 delivery of substrates to the chaperonin. Nat. Struct. Mol. Biol. 15 (8), 858–864.

Daikoku, T., Kudoh, A., Sugaya, Y., Iwahori, S., Shirata, N., Isomura, H., Tsurumi, T., 2006. Postreplicative mismatch repair factors are recruited to Epstein–Barr virus replication compartments. J. Biol. Chem. 281 (16), 11422–11430.

De Francesco, R., Migliaccio, G., 2005. Challenges and successes in developing new therapies for hepatitis C. Nature 436 (7053), 953–960.

Dworniczak, B., Mirault, M.E., 1987. Structure and expression of a human gene coding for a 71 kd heat shock 'cognate' protein. Nucleic Acids Res. 15 (13), 5181–5197.

Farr, G.W., Scharl, E.C., Schumacher, R.J., Sondek, S., Horwich, A.L., 1997. Chaperonin-mediated folding in the eukaryotic cytosol proceeds through rounds of release of native and nonnative forms. Cell 89 (6), 927–937.

Feldman, D.E., Spiess, C., Howard, D.E., Frydman, J., 2003. Tumorigenic mutations in VHL disrupt folding in vivo by interfering with chaperonin binding. Mol. Cell 12 (5), 1213–1224.

Fislová, T., Thomas, B., Graef, K.M., Fodor, E., 2010. Association of the influenza virus RNA polymerase subunit PB2 with the host chaperonin CCT. J. Virol. 84 (17), 8691–8699.

Frydman, J., Hartl, F.U., 1996. Principles of chaperone-assisted protein folding: differences between in vitro and in vivo mechanisms. Science 272 (5267), 1497–1502.

Garcin, D., Rochat, S., Kolakofsky, D., 1993. The Tacaribe arenavirus small zinc finger protein is required for both mRNA synthesis and genome replication. J. Virol. 67 (2), 807–812.

Goh, P.Y., Tan, Y.J., Lim, S.P., Tan, Y.H., Lim, S.G., Fuller-Pace, F., Hong, W., 2004. Cellular RNA helicase p68 relocalization and interaction with the hepatitis C virus (HCV) NS5B protein and the potential role of p68 in HCV RNA replication. J. Virol. 78 (10), 5288–5298.

Guo, J.T., Bichko, V.V., Seeger, C., 2001. Effect of alpha interferon on the hepatitis C virus replicon. J. Virol. 75 (18), 8516–8523.

Hamamoto, I., Nishimura, Y., Okamoto, T., Aizaki, H., Liu, M., Mori, Y., Abe, T., Suzuki, T., Lai, M.M., Miyamura, T., Moriishi, K., Matsuura, Y., 2005. Human VAP-B is involved in hepatitis C virus replication through interaction with NS5A and NS5B. J. Virol. 79 (21), 13473–13482.

Hansen, J.L., Long, A.M., Schultz, S.C., 1997. Structure of the RNA-dependent RNA polymerase of poliovirus. Structure 5 (8), 1109–1122.

Hara, H., Aizaki, H., Matsuda, M., Shinkai-Ouchi, F., Inoue, Y., Murakami, K., Shoji, I., Kawakami, H., Matsuura, Y., Lai, M.M., Miyamura, T., Wakita, T., Suzuki, T., 2009. Involvement of creatine kinase B in hepatitis C virus genome replication through interaction with the viral NS4A protein. J. Virol. 83 (10), 5137–5147.

Hardy, R.W., Marcotrigiano, J., Blight, K.J., Majors, J.E., Rice, C.M., 2003. Hepatitis C virus RNA synthesis in a cell-free system isolated from replicon-containing hepatoma cells. J. Virol. 77 (3), 2029–2037.

Hirano, M., Kaneko, S., Yamashita, T., Luo, H., Qin, W., Shirota, Y., Nomura, T., Kobayashi, K., Murakami, S., 2003. Direct interaction between nucleolin and hepatitis C virus NS5B. J. Biol. Chem. 278 (7), 5109–5115.

Hoofnagle, J.H., 2002. Course and outcome of hepatitis C. Hepatology 36 (5 Suppl 1), S21–S29.

Hu, J., Flores, D., Toft, D., Wang, X., Nguyen, D., 2004. Requirement of heat shock protein 90 for human hepatitis B virus reverse transcriptase function. J. Virol. 78 (23), 13122–13131.

Huang, H., Chopra, R., Verdine, G.L., Harrison, S.C., 1998. Structure of a covalently trapped catalytic complex of HIV-1 reverse transcriptase: implications for drug resistance. Science 282 (5394), 1669–1675.

Ichimura, T., Yamamura, H., Sasamoto, K., Tominaga, Y., Taoka, M., Kakiuchi, K., Shinkawa, T., Takahashi, N., Shimada, S., Isobe, T., 2005. 14-3-3 proteins modulate the expression of epithelial Na+ channels by phosphorylation-dependent interaction with Nedd4-2 ubiquitin ligase. J. Biol. Chem. 280 (13), 13187–13194.

Ikeda, M., Yi, M., Li, K., Lemon, S.M., 2002. Selectable subgenomic and genome-length dicistronic RNAs derived from an infectious molecular clone of the HCV-N strain of hepatitis C virus replicate efficiently in cultured Huh7 cells. J. Virol. 76 (6), 2997–3006.

Kampmueller, K.M., Miller, D.J., 2005. The cellular chaperone heat shock protein 90 facilitates Flock House virus RNA replication in *Drosophila* cells. J. Virol. 79 (11), 6827–6837.

Kim, S.J., Kim, J.H., Kim, Y.G., Lim, H.S., Oh, J.W., 2004. Protein kinase C-related kinase 2 regulates hepatitis C virus RNA polymerase function by phosphorylation. J. Biol. Chem. 279 (48), 50031–50041.

Kukihara, H., Moriishi, K., Taguwa, S., Tani, H., Abe, T., Mori, Y., Suzuki, T., Fukuhara, T., Taketomi, A., Maehara, Y., Matsuura, Y., 2009. Human VAP-C negatively regulates hepatitis C virus propagation. J. Virol. 83 (16), 7959–7969.

Kyono, K., Miyashiro, M., Taguchi, I., 2002. Human eukaryotic initiation factor 4AII associates with hepatitis C virus NS5B protein in vitro. Biochem. Biophys. Res. Commun. 292 (3), 659–666.

Laporte, M.G., Jackson, R.W., Draper, T.L., Gaboury, J.A., Galie, K., Herbertz, T., Hussey, A.R., Rippin, S.R., Benetatos, C.A., Chunduru, S.K., Christensen, J.S., Coburn, G.A., Rizzo, C.J., Rhodes, G., O'Connell, J., Howe, A.Y., Mansour, T.S., Collett, M.S., Pevear, D.C., Young, D.C., Gao, T., Tyrrell, D.L., Kneteman, N.M., Burns, C.J., Condon, S.M., 2008. The discovery of pyrano [3, 4-b] indole-based allosteric inhibitors of HCV NS5B polymerase with in vivo activity. ChemMedChem 3 (10), 1508–1515.

Liu, H.M., Aizaki, H., Choi, K.S., Machida, K., Ou, J.J., Lai, M.M., 2009. SYNCRIP (synaptotagmin-binding, cytoplasmic RNA-interacting protein) is a host factor involved in hepatitis C virus RNA replication. Virology 386 (2), 249–256.

Lohmann, V., Körner, F., Herian, U., Bartenschlager, R., 1997. Biochemical properties of hepatitis C virus NS5B RNA-dependent RNA polymerase and identification of amino acid sequence motifs essential for enzymatic activity. J. Virol. 71 (11), 8416–8428.

Lohmann, V., Roos, A., Körner, F., Koch, J.O., Bartenschlager, R., 2000. Biochemical and structural analysis of the NS5B RNA-dependent RNA polymerase of the hepatitis C virus. J. Viral Hepat. 7 (3), 167–174.

Manns, M.P., Wedemeyer, H., Cornberg, M., 2006. Treating viral hepatitis C: efficacy, side effects, and complications. Gut 55 (9), 1350–1359.

Meyer, A.S., Gillespie, J.R., Walther, D., Millet, I.S., Doniach, S., Frydman, J., 2003. Closing the folding chamber of the eukaryotic chaperonin requires the transition state of ATP hydrolysis. Cell 113 (3), 369–381.

Momose, F., Naito, T., Yano, K., Sugimoto, S., Morikawa, Y., Nagata, K., 2002. Identification of Hsp90 as a stimulatory host factor involved in influenza virus RNA synthesis. J. Biol. Chem. 277 (47), 45306–45314.

Moradpour, D., Bieck, E., Hügle, T., Wels, W., Wu, J.Z., Hong, Z., Blum, H.E., Bartenschlager, R., 2002. Functional properties of a monoclonal antibody inhibiting the hepatitis C virus RNA-dependent RNA polymerase. J. Biol. Chem. 277 (1), 593–601.

Moriishi, K., Matsuura, Y., 2007. Host factors involved in the replication of hepatitis C virus. Rev. Med. Virol. 17 (5), 343–354.

Murakami, K., Ishii, K., Ishihara, Y., Yoshizaki, S., Tanaka, K., Gotoh, Y., Aizaki, H., Kohara, M., Yoshioka, H., Mori, Y., Manabe, N., Shoji, I., Sata, T., Bartenschlager, R., Matsuura, Y., Miyamura, T., Suzuki, T., 2006. Production of infectious hepatitis C virus particles in three-dimensional cultures of the cell line carrying the genome-length dicistronic viral RNA of genotype 1b. Virology 351 (2), 381–392.

Naito, T., Momose, F., Kawaguchi, A., Nagata, K., 2007. Involvement of Hsp90 in assembly and nuclear import of influenza virus RNA polymerase subunits. J. Virol. 81 (3), 1339–1349.

Nakagawa, S., Umehara, T., Matsuda, C., Kuge, S., Sudoh, M., Kohara, M., 2007. Hsp90 inhibitors suppress HCV replication in replicon cells and humanized liver mice. Biochem. Biophys. Res. Commun. 353 (4), 882–888.
Nelson, H.B., Tang, H., 2006. Effect of cell growth on hepatitis C virus (HCV) replication and a mechanism of cell confluence-based inhibition of HCV RNA and protein expression. J. Virol. 80 (3), 1181–1190.
Niwa, H., Yamamura, K., Miyazaki, J., 1991. Efficient selection for high-expression transfectants with a novel eukaryotic vector. Gene 108 (2), 193–199.
Okamoto, T., Nishimura, Y., Ichimura, T., Suzuki, K., Miyamura, T., Suzuki, T., Moriishi, K., Matsuura, Y., 2006. Hepatitis C virus RNA replication is regulated by FKBP8 and Hsp90. EMBO J. 25 (20), 5015–5025.
Okamoto, T., Omori, H., Kaname, Y., Abe, T., Nishimura, Y., Suzuki, T., Miyamura, T., Yoshimori, T., Moriishi, K., Matsuura, Y., 2008. A single-amino-acid mutation in hepatitis C virus NS5A disrupting FKBP8 interaction impairs viral replication. J. Virol. 82 (7), 3480–3489.
Parent, R., Qu, X., Petit, M.A., Beretta, L., 2009. The heat shock cognate protein 70 is associated with hepatitis C virus particles and modulates virus infectivity. Hepatology 49 (6), 1798–1809.
Pietschmann, T., Lohmann, V., Rutter, G., Kurpanek, K., Bartenschlager, R., 2001. Characterization of cell lines carrying self-replicating hepatitis C virus RNAs. J. Virol. 75 (3), 1252–1264.
Pietschmann, T., Lohmann, V., Kaul, A., Krieger, N., Rinck, G., Rutter, G., Strand, D., Bartenschlager, R., 2002. Persistent and transient replication of full-length hepatitis C virus genomes in cell culture. J. Virol. 76 (8), 4008–4021.
Saito, I., Miyamura, T., Ohbayashi, A., Harada, H., Katayama, T., Kikuchi, S., Watanabe, Y., Koi, S., Onji, M., Ohta, Y., Choo, Q.L., Houghton, M., Kuo, G., 1990. Hepatitis C virus infection is associated with the development of hepatocellular carcinoma. Proc. Natl Acad. Sci. USA 87 (17), 6547–6549.
Seeff, L.B., Hoofnagle, J.H., 2003. Appendix: the National Institutes of Health Consensus Development Conference: management of hepatitis C 2002. Clin. Liver Dis. 7 (1), 261–287.
Shi, S.T., Lee, K.J., Aizaki, H., Hwang, S.B., Lai, M.M., 2003. Hepatitis C virus RNA replication occurs on a detergent-resistant membrane that cofractionates with caveolin-2. J. Virol. 77 (7), 4160–4168.
Shimakami, T., Honda, M., Kusakawa, T., Murata, T., Shimotohno, K., Kaneko, S., Murakami, S., 2006. Effect of hepatitis C virus (HCV) NS5B-nucleolin interaction on HCV replication with HCV subgenomic replicon. J. Virol. 80 (7), 3332–3340.
Shirakura, M., Murakami, K., Ichimura, T., Suzuki, R., Shimoji, T., Fukuda, K., Abe, K., Sato, S., Fukasawa, M., Yamakawa, Y., Nishijima, M., Moriishi, K., Matsuura, Y., Wakita, T., Suzuki, T., Howley, P.M., Miyamura, T., Shoji, I., 2007. E6AP ubiquitin ligase mediates ubiquitylation and degradation of hepatitis C virus core protein. J. Virol. 81 (3), 1174–1185.
Suzuki, T., Ishii, K., Aizaki, H., Wakita, T., 2007. Hepatitis C viral life cycle. Adv. Drug Deliv. Rev. 59 (12), 1200–1212.
Taguwa, S., Okamoto, T., Abe, T., Mori, Y., Suzuki, T., Moriishi, K., Matsuura, Y., 2008. Human butyrate-induced transcript 1 interacts with hepatitis C virus NS5A and regulates viral replication. J. Virol. 82 (6), 2631–2641.
Taguwa, S., Kambara, H., Omori, H., Tani, H., Abe, T., Mori, Y., Suzuki, T., Yoshimori, T., Moriishi, K., Matsuura, Y., 2009. Cochaperone activity of human butyrate-induced transcript 1 facilitates hepatitis C virus replication through an Hsp90-dependent pathway. J. Virol. 83 (20), 10427–10436.
Tian, G., Vainberg, I.E., Tap, W.D., Lewis, S.A., Cowan, N.J., 1995. Specificity in chaperonin-mediated protein folding. Nature 375 (6528), 250–253.
Tu, H., Gao, L., Shi, S.T., Taylor, D.R., Yang, T., Mircheff, A.K., Wen, Y., Gorbalenya, A.E., Hwang, S.B., Lai, M.M., 1999. Hepatitis C virus RNA polymerase and NS5A complex with a SNARE-like protein. Virology 263 (1), 30–41.
Ujino, S., Yamaguchi, S., Shimotohno, K., Takaku, H., 2009. Heatshock protein 90 is essential for stabilization of the hepatitis C virus nonstructural protein NS3. J. Biol. Chem. 284 (11), 6841–6846.
Valpuesta, J.M., Martín-Benitoa, J., Gómez-Puertasa, P., Carrascosaa, J.L., Willison, K.R., 2002. Structure and function of a protein folding machine: the eukaryotic cytosolic chaperonin CCT. FEBS Lett. 529 (1), 11–16.
Wakita, T., Pietschmann, T., Kato, T., Date, T., Miyamoto, M., Zhao, Z., Murthy, K., Habermann, A., Krausslich, H.G., Mizokami, M., Bartenschlager, R., Liang, T.J., 2005. Production of infectious hepatitis C virus in tissue culture from a cloned viral genome. Nat. Med. 11 (7), 791–796.
Watashi, K., Ishii, N., Hijikata, M., Inoue, D., Murata, T., Miyanari, Y., Shimotohno, K., 2005. Cyclophilin B is a functional regulator of hepatitis C virus RNA polymerase. Mol. Cell 19 (1), 111–122.
Weng, L., Du, J., Zhou, J., Ding, J., Wakita, T., Kohara, M., Toyoda, T., 2009. Modification of hepatitis C virus 1b RNA polymerase to make a highly active JFH1-type polymerase by mutation of the thumb domain. Arch. Virol. 154 (5), 765–773.
Yaffe, M.B., Farr, G.W., Miklos, D., Horwich, A.L., Sternlicht, M.L., Sternlicht, H., 1992. TCP1 complex is a molecular chaperone in tubulin biogenesis. Nature 358 (6383), 245–248.
Yam, A.Y., Xia, Y., Lin, H.T., Burlingame, A., Gerstein, M., Frydman, J., 2008. Defining the TRiC/CCT interactome links chaperonin function to stabilization of newly made proteins with complex topologies. Nat. Struct. Mol. Biol. 15 (12), 1255–1262.
Yanagida, M., Miura, Y., Yagasaki, K., Taoka, M., Isobe, T., Takahashi, N., 2000. Matrix assisted laser desorption/ionization-time of flight-mass spectrometry analysis of proteins detected by anti-phosphotyrosine antibody on two-dimensional-gels of fibroblast cell lysates after tumor necrosis factor-alpha stimulation. Electorophoresis 21 (9), 1890–1898.
Yang, G., Pevear, D.C., Collett, M.S., Chunduru, S., Young, D.C., Benetatos, C., Jordan, R., 2004. Newly synthesized hepatitis C virus replicon RNA is protected from nuclease activity by a protease-sensitive factor(s). J. Virol. 78 (18), 10202–10205.

JOURNAL OF VIROLOGY, Nov. 2010, p. 11761–11770 Vol. 84, No. 22
0022-538X/10/$12.00 doi:10.1128/JVI.00638-10
Copyright © 2010, American Society for Microbiology. All Rights Reserved.

Sphingomyelin Activates Hepatitis C Virus RNA Polymerase in a Genotype-Specific Manner[▽]†

Leiyun Weng,[1] Yuichi Hirata,[2] Masaaki Arai,[3] Michinori Kohara,[2] Takaji Wakita,[4] Koichi Watashi,[4,5] Kunitada Shimotohno,[5,6] Ying He,[7] Jin Zhong,[7] and Tetsuya Toyoda[1]*

Units of Viral Genome Regulation[1] and Viral Hepatitis,[7] Institut Pasteur of Shanghai, Key Laboratory of Molecular Virology and Immunology, Chinese Academy of Sciences, 411 Hefei Road, 200025 Shanghai, People's Republic of China; Department of Microbiology and Cell Biology, Tokyo Metropolitan Institute of Medical Biology, 3-18-22 Honkomagome, Bunkyo-Ku, Tokyo 113-8613, Japan[2]; Pharmacology Laboratory, Pharmacology Department V, Mitsubishi Tanabe Pharma Corporation, 1000 Kamoshida-cho, Aoba-ku, Yokohama 227-0033, Japan[3]; Department of Virology II, National Institute of Health, 1-23-1 Toyama, Shinjuku, Tokyo 132-8640, Japan[4]; Laboratory of Human Tumor Viruses, Department of Viral Oncology, Institute for Virus Research, Kyoto University, Kyoto 606-8507, Japan[5]; and Chiba Institute of Technology, 2-17-1 Tsudamuna, Narashino, Chiba 275-0016, Japan[6]

Received 25 March 2010/Accepted 27 August 2010

Hepatitis C virus (HCV) replication and infection depend on the lipid components of the cell, and replication is inhibited by inhibitors of sphingomyelin biosynthesis. We found that sphingomyelin bound to and activated genotype 1b RNA-dependent RNA polymerase (RdRp) by enhancing its template binding activity. Sphingomyelin also bound to 1a and JFH1 (genotype 2a) RdRps but did not activate them. Sphingomyelin did not bind to or activate J6CF (2a) RdRp. The sphingomyelin binding domain (SBD) of HCV RdRp was mapped to the helix-turn-helix structure (residues 231 to 260), which was essential for sphingomyelin binding and activation. Helix structures (residues 231 to 241 and 247 to 260) are important for RdRp activation, and 238S and 248E are important for maintaining the helix structures for template binding and RdRp activation by sphingomyelin. 241Q in helix 1 and the negatively charged 244D at the apex of the turn are important for sphingomyelin binding. Both amino acids are on the surface of the RdRp molecule. The polarity of the phosphocholine of sphingomyelin is important for HCV RdRp activation. However, phosphocholine did not activate RdRp. Twenty sphingomyelin molecules activated one RdRp molecule. The biochemical effect of sphingomyelin on HCV RdRp activity was virologically confirmed by the HCV replicon system. We also found that the SBD was the lipid raft membrane localization domain of HCV NS5B because JFH1 (2a) replicon cells harboring NS5B with the mutation A242C/S244D moved to the lipid raft while the wild type did not localize there. This agreed with the myriocin sensitivity of the mutant replicon. This sphingomyelin interaction is a target for HCV infection because most HCV RdRps have 241Q.

Hepatitis C virus (HCV) has a positive-stranded RNA genome and belongs to the family *Flaviviridae* (21). HCV chronically infects more than 130 million people worldwide (34), and HCV infection often induces liver cirrhosis and hepatocellular carcinoma (19, 28). To date, pegylated interferon (PEG-IFN) and ribavirin are the standard treatments for HCV infection. However, many patients cannot tolerate their serious side effects. Therefore, the development of new and safer therapeutic methods with better efficacy is urgently needed.

Lipids play important roles in HCV infection and replication. For example, the HCV core associates with lipid droplets and recruits nonstructural proteins and replication complexes to lipid droplet-associated membranes which are involved in the production of infectious virus particles (24). HCV RNA replication depends on viral protein association with raft membranes (2, 30). The association of cholesterol and sphingolipid with HCV particles is also important for virion maturation and infectivity (3). The inhibitors of the sphingolipid biosynthetic pathway, ISP-1 and HPA-12, which specifically inhibit serine palmitoyltransferase (SPT) (23) and ceramide trafficking from the endoplasmic reticulum (ER) to the Golgi apparatus (37), suppress HCV virus production in cell culture but not viral RNA replication by the JFH1 replicon (3). Other serine SPT inhibitors (myriocin and NA255) inhibit genotype 1b replication (4, 29, 33). Very-low-density lipoprotein (VLDL) also interacts with the HCV virion (15).

Sakamoto et al. reported that sphingomyelin bound to HCV RNA-dependent polymerase (RdRp) at the sphingomyelin binding domain (SBD; amino acids 230 to 263 of RdRp) to recruit HCV RdRp on the lipid rafts, where the HCV complex assembles, and that NA255 suppressed HCV replication by releasing HCV RdRp from the lipid rafts (29). In the present study, we analyzed the effect of sphingomyelin on HCV RdRp activity *in vitro* and found that sphingomyelin activated HCV RdRp activity in a genotype-specific manner. We also determined the sphingomyelin activation domain and the activation mechanism. Finally, we confirmed our biochemical data by a HCV replicon system.

* Corresponding author. Mailing address: Unit of Viral Genome Regulation, Institut Pasteur of Shanghai, Chinese Academy of Sciences, 411 Hefei Road, 200025 Shanghai, People's Republic of China. Phone and fax: 86 21 6385 1621. E-mail: ttoyoda@amber.plala.or.jp.

† Supplemental material for this article may be found at http://jvi.asm.org.

▽ Published ahead of print on 15 September 2010.

MATERIALS AND METHODS

HCV RNA polymerase. A C-terminal 21-amino-acid deletion was made to the HCV RdRps of strains HCR6 (genotype 1b) (36), NN (1b) (35), Con1 (1b) (5), JFH1 (2a) (36), J6CF (2a) (25), H77 (1a) (7), and RMT (1a), and the mutants

were purified from bacteria as described previously (36). HCR6 (1b) RdRp with the mutation L245A [RdRp(L245A)] or I253A [RdRp(I253A)] or the double mutation L245A and I253A [RdRp(L245A/I253A)]; JFH1 (2a) RdRp with the mutation(s) A242C/S244D, A242, S244D, or T251Q; J6CF (2a) RdRp with the mutation(s) R241Q, S244D, or R241Q/S244D; and H77 (1a) RdRp(A238S/Q248E) were introduced using an *in vitro* mutagenesis kit (Stratagene) and the oligonucleotides listed in Table S1 in the supplemental material. HCR6 (1b) His_6-tagged RdRp(L245A/I253A) was removed from pET21b/KM (36) and cloned into the BamHI/XhoI site of pGEX-6P-3 (GE), resulting in pGEXHCVHCR6RdRp(L245A/I253A).

***In vitro* HCV transcription.** *In vitro* HCV transcription was performed as described previously (36). Briefly, following 30 min of preincubation without ATP, CTP, or UTP, 100 nM HCV RdRp was incubated in 50 mM Tris-HCl (pH 8.0), 200 mM monopotassium glutamate, 3.5 mM $MnCl_2$, 1 mM dithiothreitol (DTT), 0.5 mM GTP, 50 μM ATP, 50 μM CTP, 5 μM [α-^{32}P]UTP, 200 nM RNA template (SL12-1S), 100 U/ml human placental RNase inhibitor, and the lipid (amount indicated below) at 29°C for 90 min. ^{32}P-labeled RNA products were subjected to 6% polyacrylamide gel electrophoresis (PAGE) containing 8 M urea. The resulting autoradiograph was analyzed with a Typhoon Trio plus image analyzer (GE).

RNA filter binding assay. An RNA filter binding assay was performed as described previously (36). Briefly, 100 nM HCV RdRp and 100 nM ^{32}P-labeled RNA template (SL12-1S) were incubated with or without 0.01 mg/ml egg yolk sphingomyelin in 25 μl of 50 mM Tris-HCl (pH 7.5), 200 mM monopotassium glutamate, 3.5 mM $MnCl_2$, and 1 mM DTT at 29°C for 30 min. After incubation, the solutions were diluted with 0.5 ml of TE (50 mM Tris-HCl [pH 7.5], 1 mM EDTA) buffer and filtered through nitrocellulose membranes (0.45-μm pore size; Millipore). The filter was washed five times with TE buffer, and the bound radioisotope was analyzed by Typhoon Trio plus after being dried.

Enzyme-linked immunosorbent assay (ELISA). Ninety-six-well microtiter plates (Corning) were coated with 250 ng of egg yolk sphingomyelin in ethanol by evaporation at room temperature. After the wells were blocked with phosphate-buffered saline (PBS) and 3% bovine serum albumin (BSA), they were incubated with 1 pmol of the HCV RdRp of HCR6 (1b) wild type (wt) or L245A, I253A, or L245A/I253A mutant; NN (1b); H77 (1a); RMT (1a); J6CF (2a); or JFH1 (2a) wt or A242C/S244D, A242, S244D, or T251Q mutant in Tris-buffered saline (50 mM Tris-HCl [pH 7.5] and 150 mM NaCl) for 1.5 h at room temperature. After being blocked with 3% BSA, the bound HCV RdRp was detected by adding rabbit anti-HCV RdRp serum (1:5,000) (see Fig. S1 in the supplemental material) (17) before incubation with a horseradish peroxidase (HRP)-conjugated anti-rabbit IgG antibody (1:5,000; Southern Biotech). The optical density at 450 nm (OD_{450}) was measured with a Spectra Max 190 spectrophotometer (Molecular Devices) using a TMB (3,3′,5,5′-tetramethylbenzidine) Liquid Substrate System (Sigma).

HCV subgenomic replicon. A D244S mutation was introduced into the HCV strain NN (1b) subgenomic replicon pLMH14 (35), resulting in pLMH(NN)5B(D244S) [where 5B(D244S) is the NS5B protein with the mutation D244S]. The A242C/S244D mutation was introduced into the HCV JFH1 (2a) replicon, pSGR-JFH1/luc (25), resulting in pSGR-JFH1/luc5B(A242C/S244D). The HpaI and XbaI fragment of pSGR-JFH1 (18) was replaced with that of pSGR-JFH1/luc5B(A242C/S244D), resulting in pSGR-JFH15B(A242C/S244D). The A238S/Q248E mutation was introduced into HCV H77 (1a) replicon pHCVrep13(S2204I)/Neo (7) after the neomycin gene was replaced by the firefly luciferase gene [pH77(I)/luc] by insertion of AflII and AscI sites (see Table S1 in the supplemental material), resulting in pH77(I)/luc5B(A238S/Q248E). Subgenomic replicon RNA was transcribed *in vitro* by T7 RNA polymerase using MegaScript (Ambion) after the replicon plasmids were linearized by XbaI (strain NN and JFH1 replicons) or HpaI (strain H77 replicon). Subgenomic replicon RNA was stored at −80°C after being purified by phenol-chloroform extraction and ethanol precipitation.

Replicon assay with myriocin. Huh7.5.1 cells were kindly provided by F. Chisari and were maintained in Dulbecco's modified Eagle's medium (DMEM; Gibco) with 10% fetal bovine serum (FBS; Gibco) (38). HCV replicon RNA (10 μg) was transfected into 4 × 10^6 Huh7.5.1 cells (1 × 10^7/ml) in OptiMEM I (Gibco) by electroporation (GenePulser Xcell; Bio-Rad) at 270 V, 100 Ω, and 950 μF. After transfection, the cells were plated in 12-well plates incubated in DMEM–10% FBS. At 6 h after transfection, cells were treated with 0, 5, and 50 nM myriocin. At 4, 54, and 78 h after transfection (48 and 72 h after myriocin treatment), the cells were harvested, and luciferase activity was measured using a Dual-Glo luciferase assay kit and a GloMax 96 Microplate Luminometer (Promega). Luciferase activity was normalized against the activity at 4 h after transfection (26).

HCV JFH1 wt and NS5B(A242C/S244D) replicon cells. Huh7/scr cells were kindly provided by F. Chisari of the Scripps Research Institute and were maintained in Dulbecco's modified Eagle's medium (Gibco) with 10% fetal bovine serum (Gibco). RNA (10 μg each) from SGR-JFH1 and SGR-JFH1 with the mutations A242C/S244D in NS5B [NS5B(A242C/S244D) was transfected into 4 × 10^6 Huh7/scr cells (1 × 10^7/ml) in OptiMEM I (GIBCO) by electroporation (GenePulser Xcell; Bio-Rad) at 270 V, 100 Ω, and 950 μF. After transfection, the cells were plated in 10-cm dishes and incubated in DMEM–10% FBS with 1.0 and 0.5 mg/ml G418 (Gibco). JFH1 wt and NS5B(A242C/S244D) replicon cells were maintained in DMEM–10% FBS and 0.5 mg/ml G418.

Membrane floating assay. JFH1 wt and NS5B(A242C/S244D) replicon cells were suspended in two packed cell volumes of hypotonic buffer (10 mM HEPES-NaOH [pH 7.6], 10 mM KCl, 1.5 mM $MgCl_2$, 2 mM DTT, and 1 tablet/25 ml of EDTA-free protease inhibitor cocktail tablets [Roche]) and disrupted by 30 strokes of homogenization in a Dounce homogenizer using a tight-fitting pestle at 4°C. After nuclei were removed by centrifugation at 2,000 rpm for 10 min at 4°C, the supernatant (postnuclear supernatant [PNS]) was treated with 1% Triton X-100 in TNE buffer (25 mM Tris-HCl [pH 7.6] 150 mM NaCl, 1 mM EDTA) for 30 min on ice. The lysates were supplemented with 40% sucrose and centrifuged at 38,000 rpm in a Beckman SW41 Ti rotor (Beckman Coulter) overlaid with 30% and 10% sucrose in TNE buffer at 4°C for 14 h.

Western blotting. Western blotting using anti-HCV RdRp (17), rabbit anti-NS3 (32), anti-NS5A (16) and anti-caveolin-2 was performed as previously published (17).

Reagent. Egg yolk sphingomyelin, cholesterol phosphocholine, myriocin, and rabbit anti-caveolin-2 antibodies were purchased from Sigma. Hexanoyl sphingomyelin, C_6-ceramide, C_8-β-D-glucosyl ceramide, and C_8-β-D-lactosyl ceramide were purchased from Avanti Polar Lipids. [α-^{32}P]UTP was purchased from New England Nuclear.

Statistical analysis. Significant differences were evaluated using P values calculated from a Student's t test.

Nucleotide sequence accession number. The sequence of HCV RMT has been deposited in the GenBank under accession number AB520610.

RESULTS

Sphingomyelin activation of HCV RNA polymerases of various genotypes. There are several sequence variations in the sphingomyelin binding domain (SBD; amino acids 231 to 260 of HCV RdRp) among HCV genotypes (see Fig. 7A). In order to compare the RdRps of different genotypes of HCV, we purified RdRp from genotypes 1b (strains HCR6, NN, and Con1), 1a (H77 and MRT), and 2a (JFH1 and J6CF) (see Fig. S2 in the supplemental material). First, the effect of ethanol on HCV HCR6 (1b) RdRp transcription was examined because lipids were suspended in ethanol before they were added to the HCV transcription reaction mixture. We found that 2% ethanol did not inhibit HCV transcription (see Fig. S3 in the supplemental material); therefore, all subsequent experiments were performed using less than 2% ethanol.

The kinetics of sphingomyelin activation were analyzed using egg yolk sphingomyelin for HCR6 (1b) RdRp wt (Fig. 1A) and subtype 2a (JFH1 and J6CF) RdRps (Fig. 1B), and *N*-hexanoyl-D-*erythro*-sphingosylphosphorylcholine (hexanoyl sphingomyelin) was used for HCR6 (1b) RdRp wt (Fig. 1C) and subtype 1a (H77 and RMT) RdRps (Fig. 1D). The egg yolk sphingomyelin activation curve of HCR6 (1b) RdRp wt at low concentrations (<0.01 mg/ml) was sigmoid. The transcription activity of HCR6 (1b) RdRp wt increased in a dose-dependent manner. It was activated 11-fold at 0.01 mg/ml and then plateaued (14-fold activation) at 0.1 mg/ml. However, JFH1 (2a) and J6CF (2a) RdRps were activated 2.5-fold and 2.2-fold, respectively, at 0.01 mg/ml sphingomyelin, at which point they plateaued.

Egg yolk sphingomyelin is a mixture. In order to obtain the optimal molar ratio for sphingomyelin activation of HCR6 (1b)

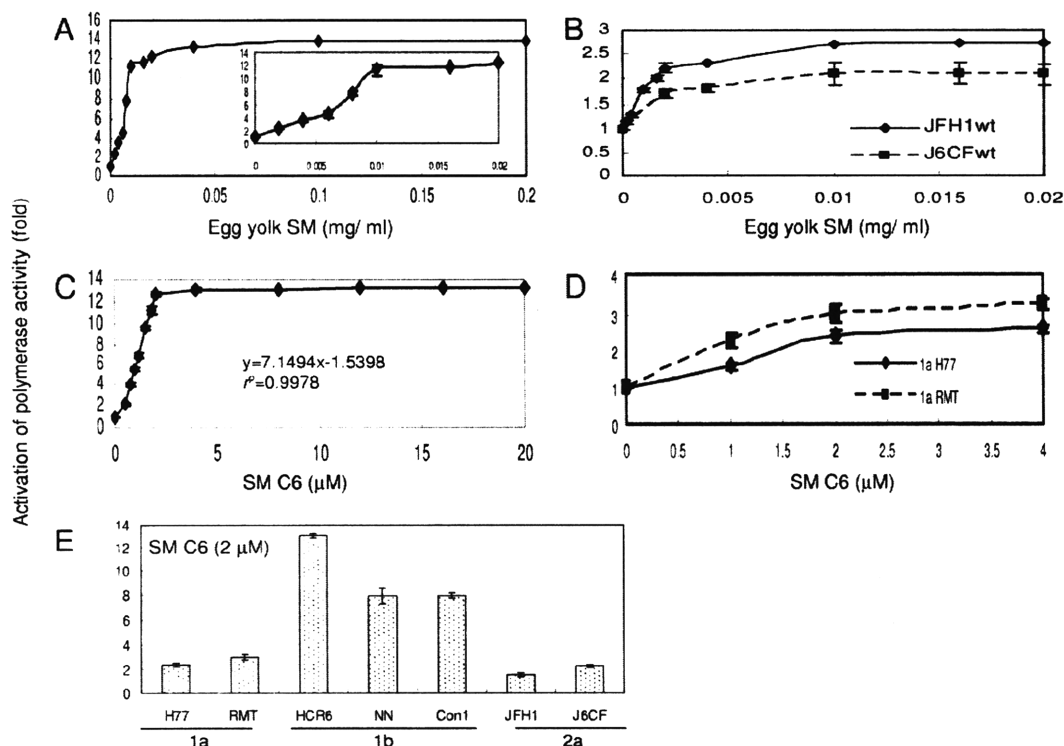

FIG. 1. Sphingomyelin activation of HCV RNA polymerases. (A) Activation kinetics of HCV HCR6 (1b) RdRp wt by egg yolk sphingomyelin (SM). The inset shows activation produced by 0 to 0.02 mg/ml egg yolk sphingomyelin. Activation kinetics of HCV 2a (JFH1 and J6CF) RdRps by egg yolk sphingomyelin (B) and of HCV HCR6 (1b) RdRp wt by hexanoyl sphingomyelin (SM C6) (C). In panel C, the first order of the graph was fitted by linear regression; the calculated equation is indicated in the graph. (D) Activation kinetics of HCV 1a (H77 and RMT) RdRps by hexanoyl sphingomyelin. (E) Activation effect of hexanoyl sphingomyelin on HCV RdRp of various genotypes. HCV RdRp (100 nM) was incubated with or without 2 μM SM C6. The names of the RdRps are indicated below the graph. Mean ± standard deviation of the activation ratio was calculated from three independent experiments.

RdRp wt, its activation kinetics were calculated using hexanoyl sphingomyelin (Fig. 1C, SM C6). The equation for the first-order ratio of hexanoyl sphingomyelin activation according to linear regression fitting was as follows: $y = 7.1494x - 1.5398$, where y is the activation ratio and x is the sphingomyelin concentration ($r^2 = 0.9978$). RdRp activation had almost plateaued at 2 μM hexanoyl sphingomyelin. The activation kinetics of JFH1 (2a) and J6CF (2a) RdRps in egg yolk sphingomyelin were biphasic and plateaued at 0.01 mg/ml. Those of RMT (1a) and H77 (1a) RdRps in hexanoyl sphingomyelin were also biphasic and plateaued at 2 μM. The curve of the first order was fitted by linear regression. The molar ratio of RdRp to hexanoyl sphingomyelin at its plateau was calculated as 1:20.

Because RdRp activation had almost plateaued at 2 μM hexanoyl sphingomyelin, we compared the effect of sphingomyelin on 100 M concentrations of RNA polymerases of the HCV 1a, 1b, and 2a genotypes using 2 μM hexanoyl sphingomyelin (Fig. 1E and Table 1).

Helix-turn-helix structure for sphingomyelin binding and activation. Sphingomyelin binds to the SBD peptide (see HCV SBD in Fig. 7) (29). Initially, we tested whether SBD was the sphingomyelin binding site in HCV RdRp by ELISA (Fig. 2A and Table 1). When the L245 and I253 residues of the SBD peptide were mutated to A, sphingomyelin binding activity was lost (29). We introduced the same mutations in HCV HCR6 (1b) RdRp and purified HCR6 (1b) RdRp with mutations L245A, I253A, and L245A/I253A. Because the C-terminal His-tagged HCR6 RdRp(L245A/I253A) was not soluble, it was solubilized by tagging of glutathione *S*-transferase (GST) sequence at the N terminus but lost polymerase activity. As the L245A/I253A mutant had lost its polymerase activity, polymerase activation was tested only for L245A and I253A (Fig. 2B and Table 1). These results confirmed that SBD located in the finger domain (residues 230E to 263G) successfully achieved sphingomyelin binding in HCV RdRp and that sphingomyelin did not bind to the SBD when the helix-turn-helix structure had been destroyed by the L245A or I253A mutation (29).

The sphingomyelin binding activities of genotype 1a and 2a RdRps were also tested (Fig. 2 and Table 1). Both JFH1 and J6CF were tested for genotype 2a because J6CF (2a) RdRp had an additional amino acid difference at position 241 in the SBD, and its sphingomyelin binding activity was very low (Fig. 2A and 7A; Table 1). J6CF (2a) RdRp(R241Q) showed the same sphingomyelin binding activity as HCR6 (1b) RdRp wt, indicating that 241Q was the critical amino acid for sphingomyelin binding. J6CF (2a) RdRp(S244D) and RdRp(R241Q/S244D) also showed higher sphingomyelin binding activity

TABLE 1. Summary of sphingomyelin activation of HCV RNA polymerase activities

Parameter	Value for the parameter by RdRp genotype, strain, and variant[a]																		
	1b							1a			2a								
	HCR6					NN	Con1	RMT	H77		J6CF				JFH1				
	wt	L245A	I253A	L245A/I253A	D244S	wt	wt	wt	wt	A238S/Q248E	wt	R241Q	S244D	R241Q/S244D	wt	A242C	S244D	A242C/S244D	T251Q
SM binding (%)[b]	100	24.3	30.8	15.5	78.7	93.4	117	144	86.7	82.5	19.3	118	53.1	80.2	70.4	75.5	93.1	92.4	80.7
Activation of polymerase (*n*-fold)[c]	13.0 (11.2)[d]	(2.8)[d]	(2.5)[d]	ND	3.6	7.9	7.9	3.0	2.0	8.1	2.3	4.3	5.6	3.4	1.6	1.0	3.1	4.4	1.8
Activation of RNA binding (*n*-fold)[c]	4.5	2.6	1.7	ND	1.9	ND	ND	ND	1.4	3.3	1.5	3.6	3.2	1.7	1.3	ND	ND	1.4	ND

[a] Numbers were averaged from three independent experiments. ND, not done.
[b] Egg yolk sphingomyelin (SM; 250 ng) was used.
[c] Hexanoyl sphingomyelin (2 μM) was used.
[d] Egg yolk sphingomyelin (0.01 mg/ml) was used.

than the wt ($P < 0.001$) but lower binding than the R241Q mutant. However, S244D showed higher RdRp activation than R241Q ($P < 0.005$), while the RdRp activation ratio of the double mutant (R241Q/S244D) was lower than that of S244D or R241Q, although all of them activated RdRp with sphingomyelin ($P < 0.005$) (Fig. 2A and C and Table 1). For JFH1, when the JFH1 RdRp SBD was modified (A242C/S244D) to allow it to bind with more sphingomyelin than the wt ($P < 0.005$), the mutant JFH1 RdRp(A242C/S244D) was activated more than the wt by sphingomyelin ($P < 0.005$) (Fig. 2A and C; Table 1). The sphingomyelin binding activity of JFH1 RdRp(T251Q) was 80.7% of that of HCR6 (1b), and its activation ratio was 1.8-fold. These results agree that SBD is both the sphingomyelin activation and binding domain and that the domains for these two activities are somehow different.

We determined which amino acid, 242C or 244D, enhanced sphingomyelin binding by comparing HCR6 (1b) and JFH1 (2a) RdRps. Sphingomyelin binding of HCR6 (1b) RdRp(D244S) was 79% of that of the wt ($P < 0.005$) (Fig. 2A and Table 1), and its activation by sphingomyelin was only 3.6-fold (Fig. 2C and Table 1). The sphingomyelin binding of JFH1 (2a) RdRp(A242C) and RdRp(S244D) increased to 75.5% and 93.1%, respectively, of HCR6 (1b) RdRp wt (Fig. 2A and Table 1). This was significantly higher than that of JFH1 (2a) RdRp wt ($P < 0.005$), and the sphingomyelin activation of JFH1 (2a) RdRp(A242C) and RdRp(S244D) was increased 1.0-fold and 3.1-fold, respectively ($P < 0.005$) (Fig. 2C and Table 1). From these mutation analyses of the J6CF and JFH1 RdRps, we concluded that 244D enhanced sphingomyelin binding and RdRp activation.

HCV 1a RdRps were not activated even though sphingomyelin bound to them (Fig. 1E and 2A and Table 1). We then tried to elucidate the domains responsible for sphingomyelin activation. There are 14 amino acids (residues 19, 25, 81, 111, 120, 131, 184, 270, 272, 329, 436, 464, 487, and 540) unique to genotype 1a RdRp in the region of residues 1 to 570 and two amino acid differences unique to 1a RdRp in SBD, i.e., 238A and 248Q (see Fig. 6A). Initially, we focused on the SBD and introduced the A238S and Q248E mutations into the H77 (2a) RdRp SBD (Fig. 2A and D and Table 1). The sphingomyelin binding activity of H77 (2a) RdRp(A238S/Q248E) was similar to that of H77 (2a) RdRp wt. The sphingomyelin activation ratio of H77 (2a) RdRp(A238S/Q248E) was increased 8.1-fold, leading us to conclude that these mutations are essential to sphingomyelin activation.

Effect of lipids on HCV RNA polymerase activity. In order to elucidate the structure of the lipids involved in activation of HCV RdRp, D-lactosyl-β-1,1′-*N*-octanoyl-D-*erythro*-sphingosine [C_8-lactosyl(β) ceramide], D-glucosyl-β1-17-N-octanoyl-D-*erythro*-sphingosine (C_8-β-D-glucosyl ceramide), *N*-hexanol-D-*erythro*-sphingosine (C_6-ceramide), and cholesterol were tested for their abilities to activate RdRp. The relative polymerase activities of 100 nM HCV HCR6 (1b) RdRp activated with 0.01 mg/ml egg yolk sphingomyelin, 2 μM hexanoyl sphingomyelin, 8 μM C_8-lactosyl(β) ceramide, 12 μM C_8-β-D-glucosyl ceramide, 12 μM C_6-ceramide, and 0.02 mg/ml cholesterol were 11.2, 13.0, 5.66, 4.19, 1.12, and 2.25 of that without lipids, respectively (Fig. 3A). The amount of lipids that gave the maximum activation was calculated from the kinetics of the lipids bound to HCR6 (1b) and JFH1 (2a) RdRps (Fig. 3B and

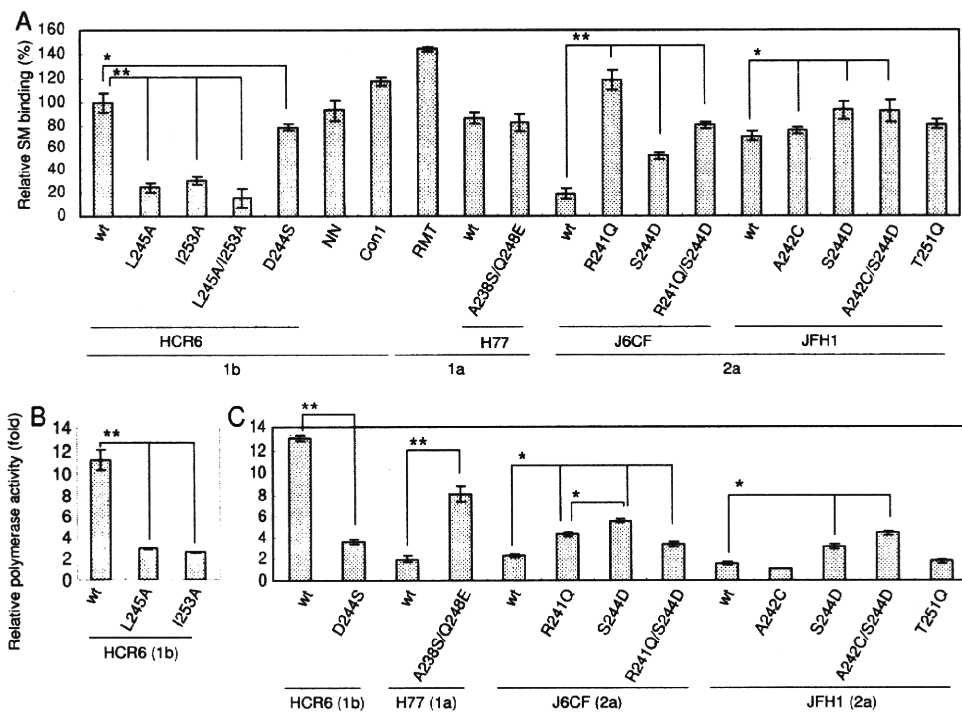

FIG. 2. Sphingomyelin binding and activation of HCV RNA polymerase sphingomyelin binding domain mutants. Names of RdRps are indicated below the graphs. (A) Egg yolk sphingomyelin (SM) binding activity relative to that of HCR6 (1b) RdRp wt. Mean ± standard deviation of the binding was calculated from three independent experiments. (B) Egg yolk sphingomyelin activation of HCR6 (1b) RdRps. RdRps (100 nM) were incubated with or without 0.01 mg/ml egg yolk sphingomyelin. (C) Hexanoyl sphingomyelin activation of the RdRps (RdRp names are indicated below the graphs). HCV RdRps (100 nM) were incubated with or without 2 μM hexanoyl sphingomyelin. The mean ± standard deviation of the activation ratio was calculated from three independent experiments. *, $P < 0.005$; ** $P < 0.001$.

C). C_8-lactosyl(β) ceramide and C_8-β-D-glucosyl ceramide activated HCR6 (1b) RdRp compared with the linear regression kinetics of the reaction with hexanoyl sphingomyelin as it plateaued (Fig. 1C and 3B). Cholesterol activated HCR6 (1b) RdRp slightly but did not activate JFH1 (2a) RdRp (Fig. 3C). We therefore concluded that the phosphocholine of sphingomyelin bound to the SBD of HCV RdRp because the order of HCV RdRp activation was hexanoyl sphingomyelin > C_8-lactosyl(β) ceramide > C_8-β-D-glucosyl ceramide, and C_6-ceramide did not activate HCV HCR6 (1b) RdRp. The polarity of the phosphocholine of sphingomyelin is important for HCV RdRp activation (see Fig. S5 in the supplemental material).

In order to test whether phosphocholine activated HCV RdRp (Fig. 3D), HCR6 (1b) RdRp was incubated with 0.4, 2, 20, 100, and 400 μg and 2, 4, 11, 54, and 100 mg of phosphocholine. Up to 400 μg of phosphocholine did not affect RdRp activity, but more than 2 mg of phosphocholine inhibited RdRp activity.

Effect of sphingomyelin on the template RNA binding of HCV RNA polymerase. The mechanism of HCV RdRp activation was analyzed. RNA polymerase changes its conformation throughout the different transcription steps, and template binding is the first step of transcription (9). Therefore, the effect of sphingomyelin on template RNA binding activity was tested (Fig. 4A and Table 1). Sphingomyelin enhanced the template RNA binding of HCR6 (1b) RdRp wt but not that of JFH1 (2a), H6CF (2a), or H77 (1a) wt RdRp. When the A238S/Q248E mutation was introduced into H77 (1a) RdRp, the RNA binding was enhanced. J6CF (2a) RdRp R241Q and S244D mutants showed similar enhancement of RNA binding, but the R241Q/S244D double mutant did not. The activation effect of RNA binding of HCR6 (1b) RdRp mutants L245A, I253A, and D244S was lower than that of RdRp wt. JFH1 (2a) RdRp wt and RdRp(A242C/S244D) showed similar RNA binding activation levels. Based on a comparison of the sphingomyelin activation of HCR6 (1b) RdRp wt and its mutants which lost sphingomyelin binding with J6CF (2a) RdRp wt and the R241Q and S244D mutants and H77 (1a) RdRp wt and the A238S/Q248E mutant, we concluded that polymerase activation by sphingomyelin was induced mainly via activation of the template RNA binding of RdRp. RNA binding activity of JFH1 (2a) RdRp wt and RdRp(A242C/S244D) was almost saturated because RNA binding of these RdRps was not activated by sphingomyelin (see Fig. S4 in the supplemental material).

HCV RdRp has to be bound with sphingomyelin before or at the same time as it binds to template RNA. After RdRp had bound to the template RNA, sphingomyelin did not enhance template RNA binding strongly (Fig. 4B).

Effect of the sphingomyelin binding domain mutations for HCV replicon activity with myriocin. In order to confirm sphingomyelin activation of HCV polymerase activity in a viral replication system, HCV replicon activity of the loss-of-function mutant HCV NN (1b) NS5B(D244S) and the gain-of-